ELSEVIER

Coordination Chemistry Reviews 227 (2002) 193–216

COORDINATION CHEMISTRY REVIEWS

www.elsevier.com/locate/ccr

From neutral iminophosphoranes to multianionic phosphazenates. The coordination chemistry of imino–aza-P(V) ligands

Alexander Steiner *, Stefano Zacchini, Philip I. Richards

Department of Chemistry, University of Liverpool, Crown Street, Liverpool L69 7ZD, UK

Received 14 September 2001; accepted 2 November 2001

Contents

Abstract

This review deals with the chemistry and coordination behaviour of imino–aza phosphorus(V) ligands focussing on s- and p-block as well as Group 11 and 12 metal complexes. Imino phosphorus(V) ligands contain one or more terminal R–N=P-units, which include iminophosphoranes R_3PNR', monoanionic diiminophosphinates $[R_2P(NR')_2]^-$, dianionic triiminophosphonates $[RP(NR')_3]^{2-}$ and trianionic tetraiminophosphates $[P(NR')_4]^{3-}$. Aza-phosphorus(V) ligands feature bridging P–N=P units, which include cyclic and polymeric phosphazenes $[R_2PN]_n$. Imino–aza- phosphorus(V) ligands containing both imino and aza functions include linear diiminodiphosphazenates $[N\{R_2P(NR')_2\}_2]^-$ and multianionic poly(imino) cyclophosphazeantes such as $[N_4\{RP(NR')\}_4]^{4-}$ and $[N_3\{P(NR')_2\}_3]^{6-}$. Imino–aza phosphorus(V) ligands are assembled of three basic building blocks: the cationic tetravalent phosphonium centre (*P*), the anionic divalent amido function (*N*) and the terminally arranged R-group. The overall negative charge *Z* of the resulting ligand system is equal to the difference between the number of *P* and the number of *N*-centres: $Z = n(P) - n(N)$. Imino–aza phosphorus(V) ligands are electron rich N-donor ligands which co-ordinate via both N(imino) and N(aza) functions and have been applied in numerous metal complexes in order to stabilise low coordination numbers, unusual oxidation states and bonding modes or serve as ligands in homogeneous catalysis. The R-group provides both steric bulk and solubility in non-polar solvents. Multianionic phosphazenates feature a polydentate ligand surface, which facilitates an extremely high metal load. P=N units of iminophosphoranes and phosphazenes have acceptor properties and enhance the acidity of α-alkyl and *ortho*-aryl protons. Deprotonation of P-alkyl and P-aryl iminophosphoranes give ligand systems featuring C,N chelating sites, which are also discussed. © 2002 Published by Elsevier Science B.V.

Keywords: Phosphorus nitrgoen ligands; Phosphazenes; Multianions

* Corresponding author.
E-mail address: a.steiner@liverpool.ac.uk (A. Steiner).

0010-8545/02/$ - see front matter © 2002 Published by Elsevier Science B.V.
PII: S0010-8545(02)00012-7

1. Introduction

Imino groups (=NR) are isoelectronic to the oxo group (=O) and are able to interact via lone pairs of electrons at nitrogen with metal ions. A variety of imino analogues of p-block oxo-anions containing Group 14 [1], 15 [2], and 16 elements [3] have been utilised as ligands in coordination chemistry. The R-group at the imino function provides steric bulk to control coordination numbers and facilitates solubility in aprotic solvents. To a certain extent, it also determines the electronic properties of the ligand. This review deals with the chemistry and coordination behaviour of imino and aza phosphorus(V) ligands focussing on s- and p-block as well as Group 11 and 12 metal complexes, but it also highlights some transition metal derivatives.

Iminophosphorus(V) compounds such as iminophosphoranes **I** feature short P–N bonds. Canonic structures of ylid **Ia** and double bonded species **Ib** contribute to the multiple bond character of the P–N bond, which is electronically related to the bonding scenario in phosphonium ylides $R_3P{=}CR_2$ and phosphine oxides $R_3P{=}O$ [4].

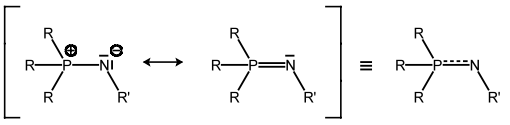

Ia **Ib** **I**

Successive replacement of R groups at phosphorus in **I** with imino functions =NR′ leads to monoanionic diiminophosphinates $[(R_2P(NR')_2]^-$ **II**, dianionic triiminophosphonates $[(RP(NR')_3]^{2-}$ **III** and trianionic tetraiminophosphates $[(P(NR')_4]^{3-}$ **IV**. These systems are isoelectronic to the corresponding oxo-anions of phosphorus, i.e. phosphinates ($H_2PO_2^-$, $R_2PO_2^-$), phosphonates (HPO_3^{2-}, RPO_3^{2-}) and phosphates (PO_4^{3-}).

P(V)-centres linked by aza functions (=N–) give neutral phosphazenes $[-(R_2)P{=}N-]_n$, which exist as polymeric or cyclic compounds, such as cyclotriphosphatriazene **V**. Phosphazenes are isoelectronic with siloxanes $[-(R_2)Si{-}O-]_n$. Their bonding mode is closely related to that of **I** with contributions from canonic forms **Va** and **Vb**:

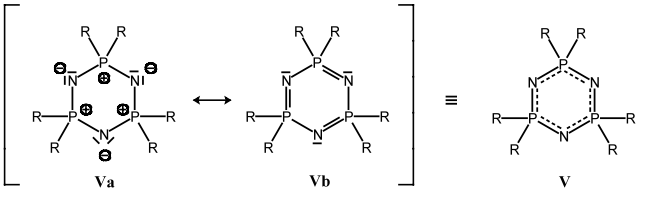

Va **Vb** **V**

Phosphorus(V) ligands featuring both bridging aza- and terminal imino-groups give negatively charged ligands, such as open chain monoanionic diiminodiphosphazenate **VI** or cyclic multianionic poly(imino)phosphazenates **VII** and **VIII**. The latter is isoelectronic with

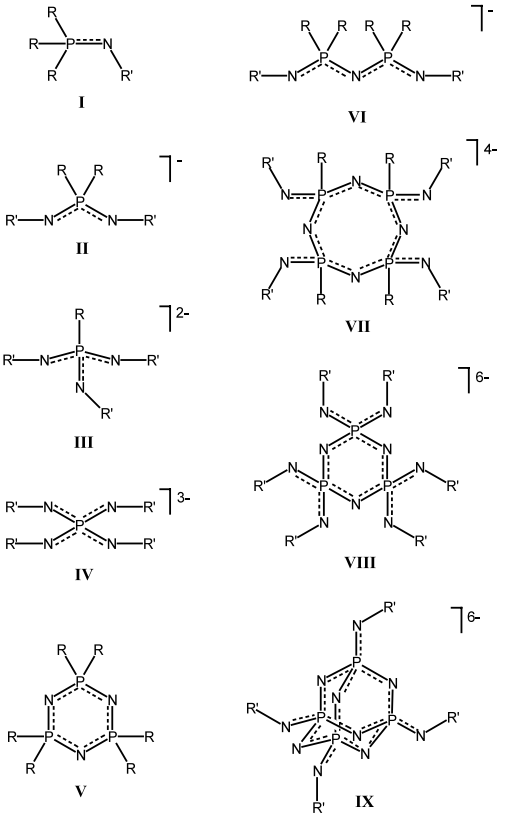

I **II** **III** **IV** **V** **VI** **VII** **VIII** **IX**

Scheme 1.

cyclotrisilicate $[Si_3O_9]^{6-}$. This account will also look at related cage-type poly(imino)phosphazenates **IX**, which, however, have been observed only within solid-state materials.

Imino- and aza- as well as mixed imino–aza-P(V) systems (see Scheme 1), are assembled out of the same construction kit, which comprises three basic building blocks: the cationic tetravalent phosphonium centre (*P*), the anionic divalent amido function (*N*) and the terminally arranged R-group (*R*). The overall negative charge, *Z*, of the resulting ligand system is equal to the difference between the number of two-connected N-centres and the number of four-connected *P*-centres.

Building blocks: 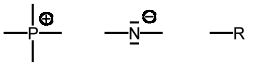

P *N* *R*

Charge: $Z = n(P) - n(N)$

Both iminophosphorane and phosphazene units have acceptor properties, which not only stabilise above systems but also enhance the acidity of α-alkyl and *ortho*-aryl protons. This again has led to a number of interesting ligand systems featuring C,N chelating sites. These systems will be discussed alongside iminophosphoranes and phosphazenes. Imino-P(V) ligands containing additional Group 16 and 17 donor atoms at P

have been reviewed elsewhere [5] and will not be discussed.

2. Imino-phosphorus(V) ligands

2.1. Iminophosphoranes

The two mainly applied synthetic routes leading to iminophosphoranes **I** are the Staudinger reaction of tertiary phosphines with organoazides under elimination of dinitrogen [6] and the Kirsanov reaction of dihalophosphoranes (X = Cl, Br) with primary amines, carried out in the presence of an auxiliary base [4].

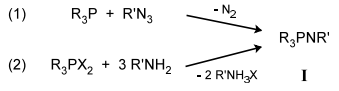

Simple iminophosphoranes act as neutral monodentate ligands via the lone pair at the nitrogen centre. Iminophosphoranes are predominantly two-electron σ-donors with only minor π-acceptor properties and are easily exchanged by other ligands [7]. Two magnesium as well as a number of Group 11 and 12 metal complexes have been structurally characterised. Magnesium complexes $\mathbf{I}_2MgI_2$ and $\mathbf{I}MgBrI(OEt_2)$ (R = Me, R′ = $SiMe_3$) are formed as side products in the reaction of $Me_3PNSiMe_3$ with Grignard reagents. Both Mg complexes are monomeric and have tetrahedral metal environments [8]. Group 11 and 12 metal halide adducts of **I** have been obtained from mixtures of metal halide salts and **I** in chlorinated hydrocarbon solvents: The **I**CuCl adduct, **1** exhibits a linear metal environment [9], whereas the corresponding $CuCl_2$ complexes exist as dimeric species $[\mathbf{I}CuCl_2]_2$ **2a** (R = Me, R′ = $SiMe_3$) [10] and **2b** (R = Ph, R′ = $SiMe_3$) [11]. Zinc halide adducts of **I** have been obtained from reaction of zinc halide with **I** in CH_2Cl_2. The zinc chloride adduct $\mathbf{I}_2ZnCl_2$ displays a monomeric coordination pattern [12], whereas the pattern of the iodide derivative $[\mathbf{I}_2ZnI_2]_2$ (R = Et, R′ = $SiMe_3$) corresponds to that of **2** [13]. The dimeric geometry of **2** is also adopted in $[\mathbf{I}_2HgCl_2]_2$ [14].

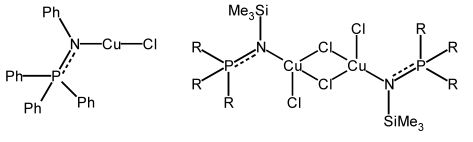

1 2

P–N bonds in **I** usually appear as very strong broad bands in the IR spectrum at around 1300 cm^{-1} [15] and are red-shifted upon metal coordination. Red-shifts between 150 and 250 wave numbers are found upon adduct formation with trialkylmetal adducts of Group 13 metals (**3**) [16].

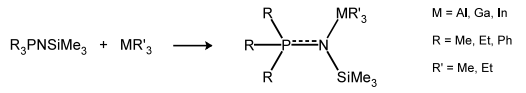

3

The controlled Staudinger reaction of diphosphines with one equivalent of azide leads to heterofunctional phosphino-iminophosphoranes [17], such as **4**, which exhibit bidentate P,N chelation sites (**4a**) and have been applied in various transition metal complexes [18]. Similarly, the phenylene derivative (**4b**) acts as a heterofunctional bidentate ligand [19]. Methylene bis(iminophosphoranes) (**5**) are obtained in a straightforward manner by treating diphosphines with two equivalents of azides [20]. In coordination sphres of transition metals, **5** exists in two tautomeric forms: it chelates either via both N sites forming six-membered metalocycles (**5a**) [21], or via N,C sites resulting in four-membered metalocycles (**5b**) [22].

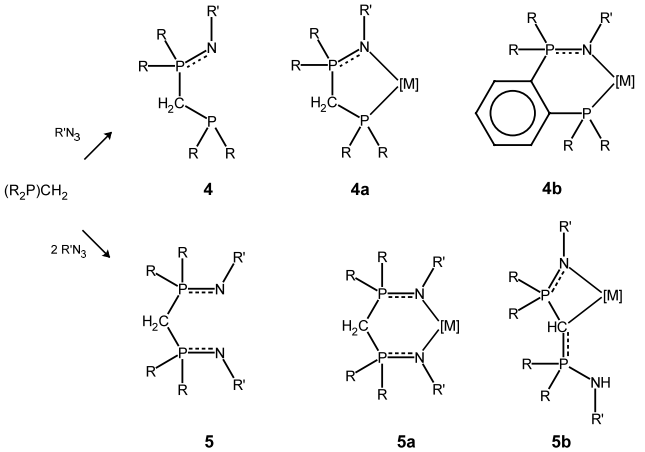

4 4a 4b

5 5a 5b

Chiral bis(iminophosphoranes) have been tested as bidentate nitrogen ligands for enantioselective catalysis. Double Kirsanov reaction of chiral diamines with Ph_3PBr_2 followed by base treatment leads to **6** and **7**. Metal complexes [**6**Rh(cod)]BF_4 and [**6**$CoCl_2$] have been structurally characterised. Copper catalysed cyclopropanation of styrene by ethyl diazoacetate using [**7**CuOTf] gives enantiomeric excess of up to 90% [23].

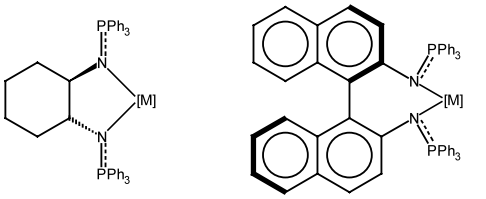

6[M] 7[M]

2.1.1. Ligands derived from α-deprotonation of P-alkyl iminophosphoranes

Similar to ketones, sulfones, hydrazones, etc. [24], P-alkyl iminophosphoranes (**8**) are moderately acidic and

are deprotonated at α-C positions by carbanionic reagents such as organolithiums. Several lithium complexes (**9**) have been obtained and structurally characterised. The negative charge in **9** is distributed over both C- and N-donor functions, as indicated by shorter P–C and slightly longer P–N bonds than observed in **I**. Lithium ions are chelated by the deprotonated ligand in a bidentate fashion by C and N centres. The steric bulk of **8** and the nature of donor additives L determine oligomerisation grades, varying from monomeric in **9a** (R^1, R^2 = Ph; R^3, R^4 = H; L = $(thf)_2$) [25] and **9b** (R^1 = Ph; R^2, R^3, $SiMe_3$; R_4 = H; L = $(Et_2O)_2$) [26], dimeric in **9c** (R^1 = Ph; R^2, R^3, $SiMe_3$; R_4 = H) and **9d** (R^1 = *i*Pr; R^2 = $SiMe_3$; R^3, R^4 = Me) [27] and tetrameric in **9e** (R^1 = Me; R^2 = $SiMe_3$; R^3, R^4 = H) and **9f** (R^1 = Et; R^2 = $SiMe_3$; R^3 = Me; R^4 = H) [28]. Cystal structures of **9a**, **9d** and **9e** are illustrated in Fig. 1. Grignard reagents EtMgBr and MeMgI deprotonate **8** correspondingly yielding $MgX(CH_2PMe_2NSiMe_3)$ (X = Br, I) [8].

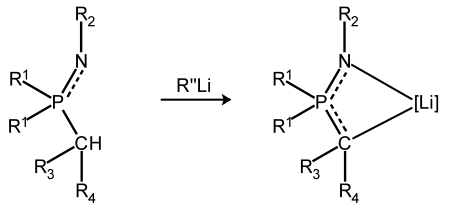

8 **9**

Reaction of **9** with various organic electrophiles, including alkylation and acylation, occur exclusively at the carbon centre [29]. **9b** undergoes transmetalation reactions with KOtBu and $PbCl_2$, respectively. The lead complex has been structurally characterised as the monomeric species **10**. The four-co-ordinate lead atom has a stereochemically active lone pair of electrons and interacts via short Pb–C (average 245 pm) and rather long Pb–N bonds (average 268 pm) [30]. **9f** reacts with CuI to form the mixed Li–Cu complex **11**, in which lithium and copper ions are both linearly co-ordinated: Li by the hard N- and Cu by the softer C-centres. Transmetalation of **9f** with equimolar amounts of $ZnCl_2$ leads to the formation of dodecanuclear zinc complex **12**, which exists as a macrocyclic structure comprising six $[Cl_2Zn_2\{CH(Me)P(Et)_2NSiMe_3\}_2]$ sub-units linked by chloride ions (Fig. 2) [28].

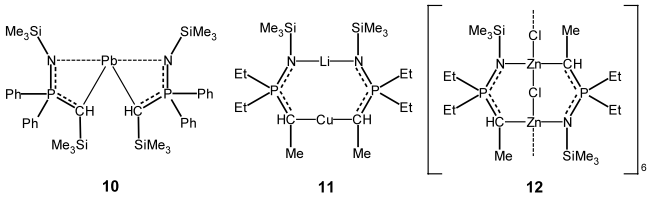

10 **11** **12**

The reaction of **9e** with $ZnCl_2$ or $CoCl_2$ in the presence of silicone grease and butyllithium leads to the formation of the mixed ligand Li_{14}-cluster complex $[Li_{14}(CHPMe_2NSiMe_3)_6(OSiMe_2Bu)_2]$ (**13**) [31] (Fig. 3).

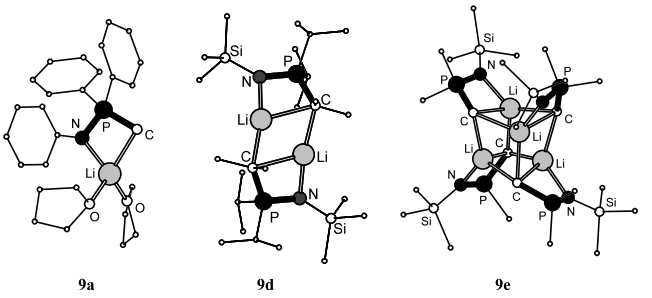

9a **9d** **9e**

Fig. 1. Crystal structures of α-lithiated P-alkyl iminophosphoranes.

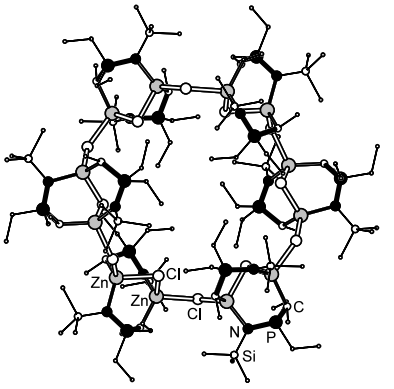

Fig. 2. Crystal structure of macrocyclic zinc complex **12**.

The monoanionic $[OSiMe_2Bu]$ units are generated by the reaction of *n*-BuLi with silicone grease, $(-Me_2SiO-)_n$. Each iminophosphorane moiety is deprotonated twice at the same methyl group. The existence of methandiide H_2C^{2-} and its derivatives RHC^{2-} and R_2C^{2-} have remained somewhat illusive due to lack of structural data and **13** is the first structurally described dilithium methanediide derivative. Each dianionic C-centre co-ordinates five lithium ions. The negative charge is delocalised onto the P–N unit as indicated by rather short P–C bonds (170 pm) and long P–N bonds (162 pm). The formation of **13** proceeds via disproportionation of monoanionic **9e** into dianionic **13** and the neutral iminophosphorane $Me_3PNSiMe_3$, which forms a donor–acceptor complex with the metal dihalide.

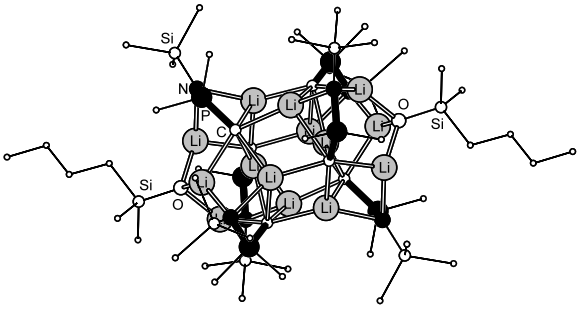

Fig. 3. Crystal structure of $[Li_{14}(CHPMe_2NSiMe_3)_6(OSiMe_2Bu)_2]$ (**13**).

The methylene protons in bis(iminophosphoranes) (**5**) are fairly acidic and single deprotonation affords monoanionic $[HC(R_2PNR')_2]^-$ (**14**), which adopts either coordination pattern **14a** or **14b** [32].

Complexes of monoanionic (**14**) with alkali metals, were generated by deprotonation of **5** with MeLi, NaH,

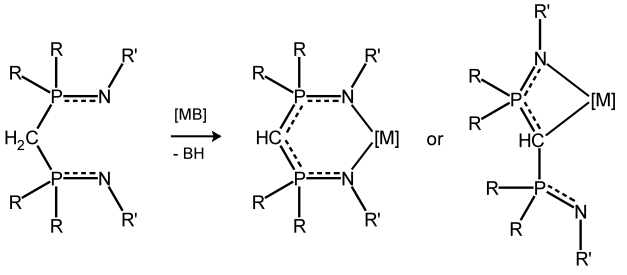

5 **14a** **14b**

and KH, respectively, and exist in both solvated monomeric (Li, Na, K) [33] and solvent-free dimeric form (Li, Na) [34]. Monomeric complexes $[(Et_2O)Li\{HC(Cy_2PNSiMe_3)\}]$ (**15**), $[(thf)_2Na\{HC(Ph_2PNSiMe_3)\}]$ (**16**) and $[(thf)_2K\{HC(Ph_2PNSiMe_3)\}]$ (**17**) exhibit coordination mode (**14a**). In addition there is a Li–C contact between the lithium ion and the CH bridge in **15** (Li···C 263.3 pm), and in **17** K is further coordinated by the π-system of one phenyl ring. Dimeric complexes of Li (**18**) (Fig. 3) and Na (**19**) were obtained donor free from **5** using alkali metal silylamides $M\{NCSiMe_3)_2\}$ as metal bases. The C atom and both N atoms of the ligand backbone are involved in metal coordination in **18** and **19**. Structural parameters of P–C and P–N bonds suggest that the negative charge is spread across the central N–P–C–P–N backbone. In addition, **18** exhibits very close contacts between lithium ions and methine protons. Trimethylaluminium as well as dimethylzinc deprotonate **5** at room temperature (r.t.) to form $Me_2Al\{HC(Ph_2PNSiMe_3)_2\}$ (**20**) [35] and $MeZn\{HC(Ph_2PNSiMe_3)_2\}$ (**21**) [36], respectively. Both complexes are monomeric in the solid state and adopt coordination mode (**14a**). **21** undergoes C–C bond formation with adamantyl isocyanate to form **22**, which contains the monoanionic tripodal ligand $[AdNC(O)C(Ph_2PNSiMe_3)_2]^-$.

It should be noted, that α-deprotonated P-alkyl iminophosphorane ligands in **9** and **14** are isoelectronic

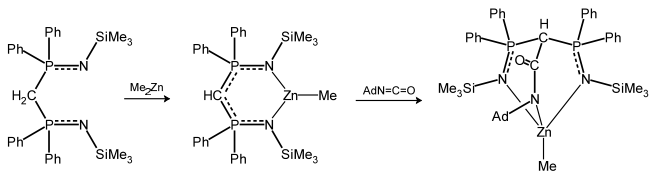

21 **22**

with monoanionic diiminophosphinate (**II**) and diiminodiphosphazenate (**VI**), respectively. One N(imino) atom in **II** or the N(aza) atom in **VI** is formally replaced

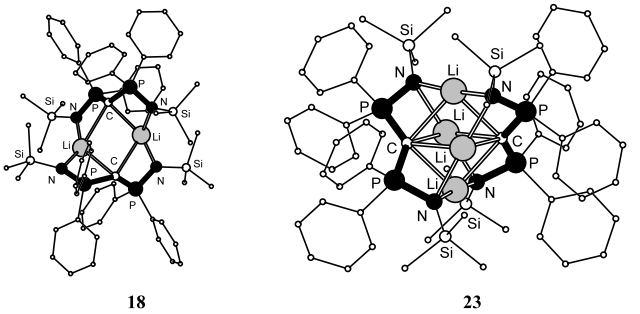

18 **23**

Fig. 4. Crystal structures of lithium methanide and -methanediide derivatives.

by a CH or CR group in α-C-deprotonated ligands. Isoelectronic complexes of corresponding N- and CH-ligands containing identical R, R′ groups and metal centres show very similar coordination pattern. Structurally characterised pairs (CH-/N-ligand) include lithium (**9b/43**), (**17/88**), lead (**10/54**) and aluminium (**20/92**) complexes (see chapters 2.2. and 4.1).

Both methylene protons in the bis(iminophosphorane) (**5**) are sufficiently acidic to be displaced directly on reaction with excess organolithiums, which represents, compared with the formation of **13**, a direct route towards methanediide derivatives. Treatment of **5** with either excess MeLi in benzene [37] or two equivalents of PhLi in toluene [38] yields the dimeric complex $[Li_2\{C(Ph_2PNSiMe_3)_2\}]_2$ (**23**). **23** contains a square arrangement of four lithium ions, which is bicapped by the doubly deprotonated C atoms. In addition each of the four nitrogen centres bridge two lithium atoms (Fig. 4). In comparison to monoanionic **18**, in **23** the P–N bonds are longer and the P–C bonds are significantly shorter (P–N (average) 159 (in **18**), 163 pm (in **23**); P–C (average) 174 (in **18**); 169 pm (in **23**)), indicating that the negative charge in **23** is highly delocalised onto both iminophosphorane units.

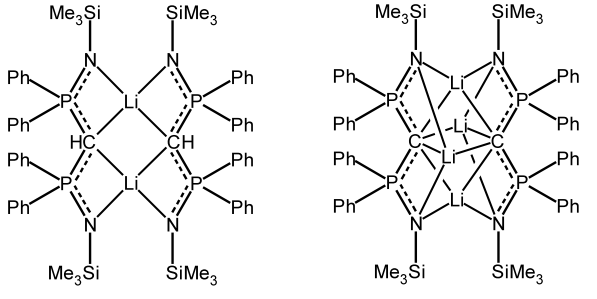

18 **23**

Correspondingly **20** is deprotonated by adding a further equivalent of Me_3Al to form the spirocyclic complex **24**. Whereas, **20** is formed rapidly by reaction of **5** with Me_3Al at r.t., the formation of **24** requires refluxing of the reaction mixture in toluene. **24** reacts with heteroallenes to form metallobicyclic compounds **25** and **26** via C=C double bond formation [39].

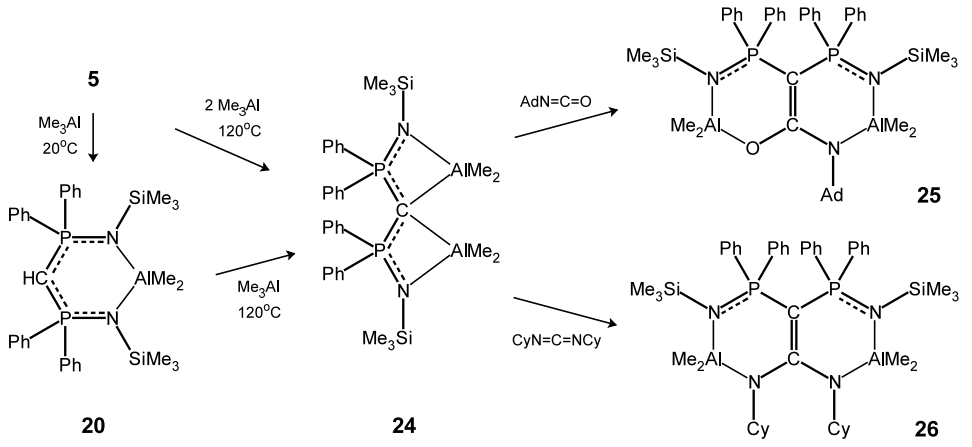

Group 14 complexes have been generated either by reaction of **18** with MCl_2 (M = Ge, Pb) or reaction of **5** with $M\{N(SiMe_3)_2\}_2$ (M = Sn, Pb) [40]. The germanium complex **27** comprises two germavinylidene units [Ge=$C(Ph_2P{=}NSiMe_3)_2$] interacting via Ge–N and Ge–Ge contacts in a head-to-head manner and exhibits two different Ge environments. Analogous Sn and Pb complexes (**28**) are dimeric with bridging methandiide centres. In all doubly deprotonated ligands the charge is delocalised across both iminophosphorane functions as indicated by shortened P–C and elongated P–N bonds.

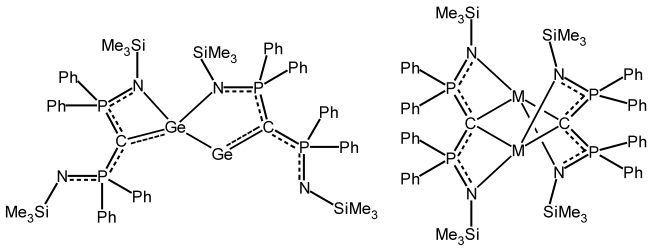

Deprotonation and/or transmetalation of **5**, **18** and **23** with transition metal halide derivatives has led to a number of carbene complexes. This area has been reviewed recently [41]. Group 4 carbene complexes have been generated either by reaction of **23** with $MCl_4(thf)_2$ (M = Ti, Zr) [42] or **5** with $MCl_2\{N(SiMe_3)_2\}_2$ (M = Zr, Hf) [43], as 'pincer' complexes (**29**). The M–C multiple bond in these compounds undergoes [2+2] cycloadditions in presence of heteroallenes RC=N=O and RN=C=NR [44]. A similar bonding mode is observed in the Sm(III) complex **30**, which has been obtained from reaction of **5** with $Sm(NCy_2)_3(thf)$ [45]. In contrast, carbene centres act in a bridging manner in the dinuclear chromium complex **31**, which has been produced by treating **23** with $CrCl_2(thf)_2$ [46].

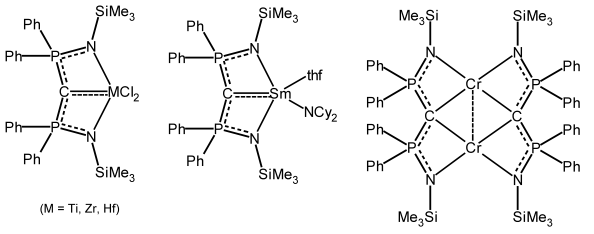

2.1.2. Ligands derived from ortho-deprotonation of P-aryl iminophosphoranes

P-phenyl derivatives of **I** are deprotonated in the *ortho*-position by strong organometallic bases. Methyllithium deprotonates one phenyl substituent in $Ph_3PNSiMe_3$ (**32**) to form the dimeric complex $[(Et_2O)Li_2\{(o\text{-}C_6H_4)(Ph)_2PNSiMe_3\}_2]$ (**33**) (Fig. 5) [47]. P–N bond lengths in **33** (156.2 pm) are only marginally longer than in **32** (154.2 pm) [48]. The P–N stretching frequency, however, undergoes a considerable red-shift of 120 cm^{-1} upon lithiation from **32** to **33**. There are two different lithium environments in **33**: one lithium ion is co-ordinated tetrahedrally by N,C chelates of both ligands involving the imino-N atom and the deprotonated aryl-C functions, whereas, the other lithium ion

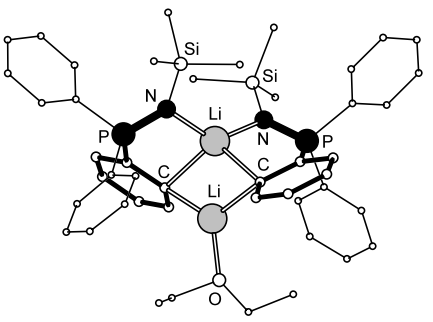

Fig. 5. Crystal structure of **33**.

interacts with the deprotonated C-functions of both ligands and one diethyl ether molecule.

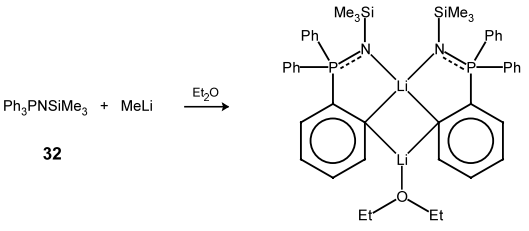

Remarkably, the corresponding tripyridyl derivative follows a completely different route upon equivalent treatment: MeLi adds to the P–N bond, while two pyridyl substituents are eliminated to undergo a C–C coupling reaction forming bipyridyl, phosphorus is reduced from oxidation state +V to +III. An X-ray structure analysis of the resulting complex **34** reveals that the bipyridyl molecule is transferred into the coordination sphere of lithium.

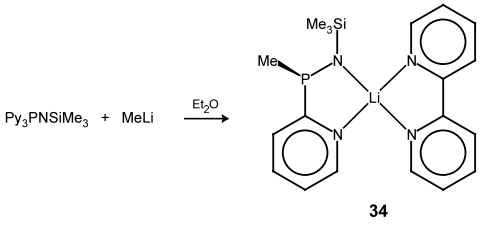

Thermolysis of the adduct complex of **32** with triphenylaluminium forms complex **35** via intramolecular *ortho*-deprotonation [49]. In contrast, the adduct complex of **32** and trimethyl aluminium dissociates upon heating.

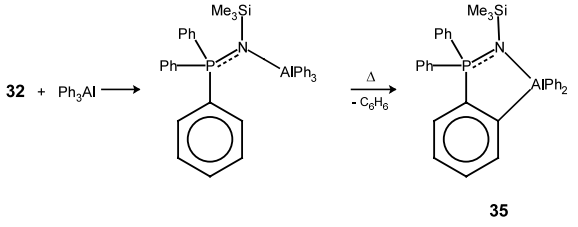

Ortho-metalation also occurs on treating Ph_3PNPh with $PhCH_2Mn(CO)_5$, leading to the formation of $[(CO)_4Mn(o\text{-}C_6H_4)(Ph)_2PNPh]$ (**36**). The Mn(I) centre in **36** is chelated by the *ortho*-deprotonated C-centre and the imino-N-atom [50]. Toluene and heptane solutions of **36** are thermochromic and change colour from golden-yellow to purple when heated to 100 °C. Transmetalation reactions of **33** with metal halides MCl_2 (M = Zn [51], Sn, Pb [52]) give metal complexes $[M\{(o\text{-}C_6H_4)(Ph)_2PNSiM_3\}_2]$ (**37**), which exhibit the familiar bidentate C,N chelation, as in **33**. Reaction of **33** with CuCl leads to the dimeric copper complex **38**. The Cu atom is almost linearly co-ordinated by C and N sites (C–Cu–N 167.8°) with additional d^{10}–d^{10}-interaction between Cu(I) ions of 248.8 pm. Reaction of **33** with $CuCl_2$ yields the biaryl compound **39** resulting via C–C coupling reaction of the deprotonated *ortho* functions.

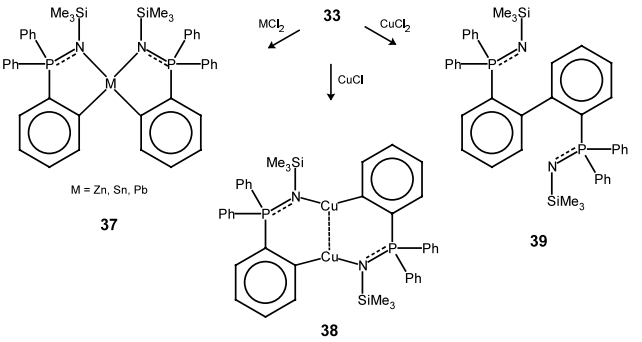

Ortho deprotonation is also considered as the initial step in the reaction of **9b** with catalytic amounts of *n*-BuLi, which leads to Si–C bond formation between one of the phenyl substituents at P and the N-silyl group under formal elimination of MeLi. MeLi again reacts in the same way with another molecule **9b** to form the bicyclic structure **40**.

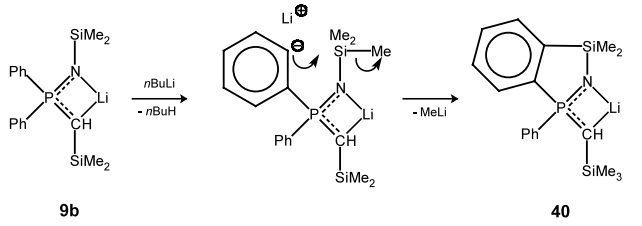

2.2. Diiminophosphinates

Monoanionic diiminophosphinates (**II**) act as monoanionic bidentate *N*,*N*′ chelating ligands and have been widely employed as both electron rich and shielding ligands in main group and transition metal chemistry. Protic ligand precursors are obtained as outlined in Scheme 2. Staudinger-type reactions of secondary phosphines with two equivalents of azide [53], or of aminophosphines with one equivalent of azide [54]

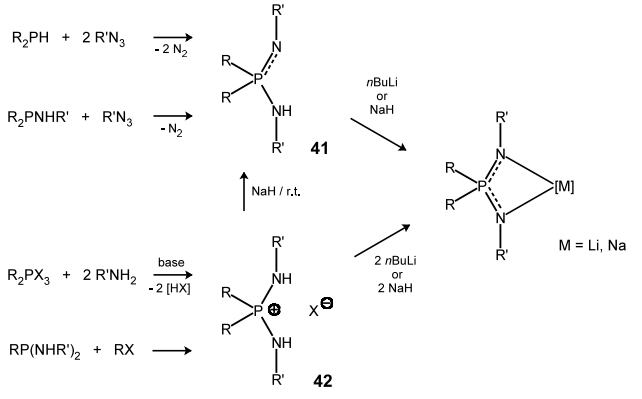

Scheme 2.

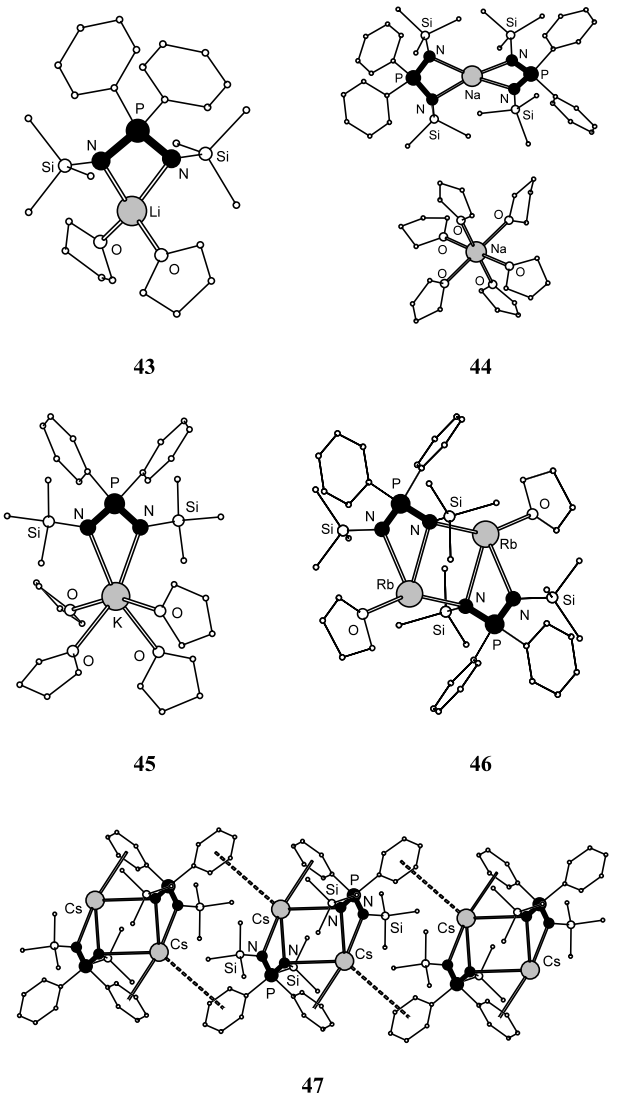

Fig. 6. Alkali metal complexes of diiminophosphinates.

lead to the aminoiminophosphorane **41** (= diiminophosphinic acid). On the other hand, aminolysis reaction of trihalophosphoranes R_3PX_2 (X = Cl, Br) with primary amines in the presence of base [55] and alkylation of diaminophosphines [56] yield diamino phosphonium salts **42**, which are converted into **41** by strong base. Deprotonation reactions with appropriate metal bases lead to desired metal complexes. Alternatively, Li and Na salts are easily prepared and are good transmetalating agents.

Complexes of all alkali [57] and alkaline earth [58] metal complexes were synthesised and characterised by X-ray crystallography (except Fr and Ra). Alkali metal complexes were synthesised by the reaction of $Ph_2P(NSiMe_3)(NHSiMe_3)$ (**41a**) with *n*-BuLi, NaH, KH, Rb, Cs and show quite non-uniform aggregation patterns in the solid-state (Fig. 6). Lithium and potassium derivatives exist as monomeric complexes $[(thf)_2Li\{Ph_2P(NSiMe_3)_2\}]$ (**43**) and $[(thf)_4K\{Ph_2P(NSiMe_3)_2\}]$ (**45**), in which the metal ions are co-ordinatively saturated by two (Li) and four (K) molecules of thf. In contrast, the sodium analogue forms the solvent separated ion pair $[Na(thf)_6][Na\{Ph_2P(NSiMe_3)_2\}_2]$ (**44**). Six thf molecules in the cationic moiety octahedrally co-ordinate one sodium ion, whereas, the other one is four co-ordinated by two diiminophosphinate ligands in a highly distorted tetrahedral fashion. **44** was the first structurally characterised sodium sodiate, in which sodium is located in both the complex cation and the complex anion of a separated ion pair. The rubidium salt (**46**) shows a dimeric motif, in which both kite shaped four membered Rb–N–P–N rings associate in head-to-tail fashion. The dimer motif also is observed in the solvent free caesium salt **47**. Intra- and intermolecular interactions between caesium ions and phenyl rings at phosphorus result in a polymeric assembly of **47** in the solid state. P–N bond lengths of alkali metal complexes are in close range (e.g. 158 pm in **43**) as ligands co-ordinate symmetrically via both N-centres. This indicates equal distribution of negative charge onto both nitrogen atoms .

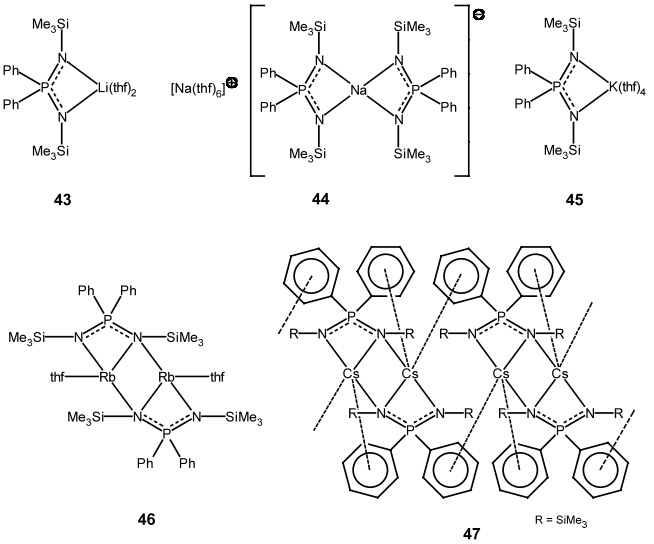

Alkaline earth metal complexes have been synthesised by deprotonation of **41a** with $M\{N(SiMe)_3\}_2$ and show, in contrast to alkali metal complexes, uniform coordination patterns. All metal ions are chelated by two ligands in monomeric complexes. Be (**48**) and Mg (**49**) complexes are homoleptic. The larger metal ions are additionally co-ordinated by one (Ca (**50**)) and two (Sr (**51**), Ba (**52**)) thf molecules. Equivalent to the symmetrical ligand pattern of alkali metal complexes, P–N bond lengths of Be, Mg, Sr and Ba compounds are within a narrow range. However, in the penta-coordinate calcium complex **50** both ligands deviate markedly from symmetrical ligand coordination. M–N bonds toward axial sites of the distorted trigonal bipyramidal coordination polyhedron are on average 15 pm longer

than those involving equatorial sites and P–N bonds within the ligand differ by 8 pm: P–N(ax) 159 pm, P–N(eq) 166 pm. This indicates that the negative charge is strongly polarised towards the equatorial N-atoms of both ligands.

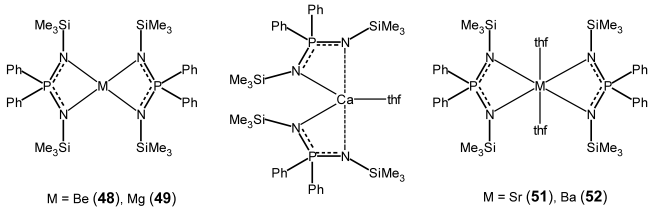

50

Group 13 metal complexes $[Me_2M\{Ph_2P(NSiMe_3)_2\}]$ (M = Al, Ga, In) **53** were prepared by treatment of **41a** with trimethylaluminium, -gallium and -indium, respectively. These compounds are thermally highly stable and partly volatile under reduced pressure. Cryoscopic molecular weight measurements suggest monomeric species [59]. Sn(II) and Pb(II) derivatives, derived from transmetalation of **43** using MCl_2 exist as monomeric compounds $[M\{Ph_2P(NSiMe_3)_2\}_2]$ (**54**). Metal centres in both complexes are four-co-ordinate and show distorted trigonal bipyramidal environments, similar to that of **50**, but with the stereoactive lone pair in equatorial position. Correspondingly, axial M–N bonds are on average 25 pm longer than equatorial M–N bonds [60]. The lead complex closely resembles its isoelectronic C,N counterpart **10**, which also shows a highly unsymmetrical coordination pattern.

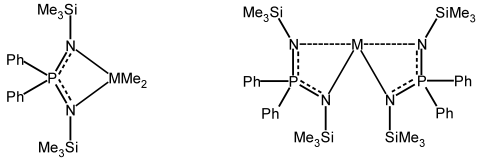

53 54

Sterically bulky diiminoanions such as **II** are regarded as ligand equivalents to pentamethylcyclopentadienide (Cp*) in terms of steric and electronic properties. In a similar manner as Cp*, the diiminophosphinate ligand stabilises ytterbium in oxidation state +II. $[(thf)_2Yb\{(Ph_2P(NSiMe_3)_2\}_2]$ (**55**) has been obtained from the reaction of **43** with YbI_2 and was characterised spectroscopically. A $^{171}Yb-^{31}P$ coupling constant of 67 Hz is observed in NMR spectra of **55**. Reaction of SmI_2 with **43** led to formation of the samarium(III) complex $[(thf)_2Li(\mu\text{-}I)_2Sm\{Ph_2P(NSiMe_3)_2\}]$, which was characterised by X-ray crystallography. Oxidation of Sm(II) occurred upon work-up due to the high reactivity of the initial product [61]. Bis(diiminophosphinates) of actinides have been reported of uranium(IV) and (VI) ($[UCl_2\{(Ph_2P(NSiMe_3)_2\}_2]$ and $\{UO_2(Ph_2P(NSiMe_3)_2\}_2]$, respectively) as well as Th(IV) ($[Cl_2Th\{(Ph_2P(NSiMe_3)_2\}_2]$ [62].

Several diiminophosphinates containing Group 4 metals have been synthesised such as chloro $[(CH_3CN)Cl_3M\{Ph_2P(NSiMe_3)_2\}]$ (M = Ti [63] Zr [64]) and imido $[t\text{-}BuN{=}Ti\{Ph_2P(NSiMe_3)_2\}_2]$ [65] compounds. With the objective to generate metallocene-like homogenous polymerisation catalysts, $[Cl_2Zr\{R_2P(NR')_2\}_2]$ and mixed $[Cl_2ZrCp\{R_2P(NR')_2\}]$ were prepared. Both act as active ethylene polymerisation catalysts in the presence of MAO providing high molecular weight poly(ethylene) with narrow molecular weight distributions [66]. $Ph_2P(NSiMe_3)N(SiMe_3)_2$ reacts with CuCl at 120 °C to give the dimeric Cu(I) complex **56**. The two diiminophosphinate ligands exhibit a bridging coordination mode towards the two linearly co-ordinated Cu(I) centres. The puckered $Cu_2N_4P_2$ eight-membered ring adopts C_2 symmetry and shows a rather long Cu···Cu distance of 262.1 pm [67].

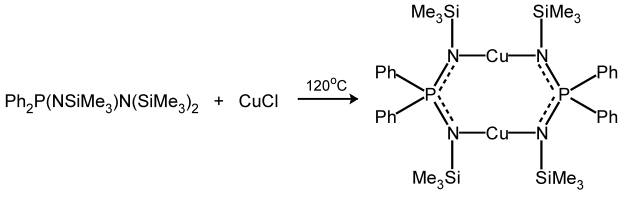

56

The steric demand and both σ- and π-donating properties of the diiminophosphinate ligand facilitate the stabilisation of the copper(I) ethylene complex **57** [68]. In contrast to otherwise quite labile Cu(I) olefin species, this complex is remarkably stable, due to increased π-backbonding to the olefin. The complex melts at 108 °C and no decomposition occurs under reduced pressure (10^{-3} mbar). Structural parameters and spectral properties of the complexed ethylene are close to those observed in free ethylene. Reaction of **57** with O_2 yields the uncharged dinuclear copper(III) bis(μ-oxo) species **58** [69]. Both **57** and **58** were characterised by X-ray diffraction.

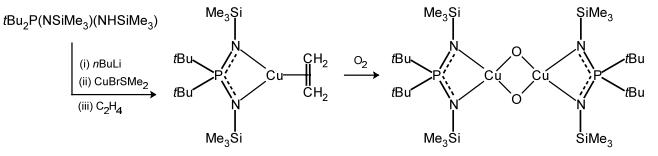

57 58

In order to generate a ligand system with ambidentate chelation sites, the dipyridiyl amino imino phosphorane (**59**) was synthesised by treatment of dipyridylphosphine with excess silylazide [70]. **59** is deprotonated by disilylamide salts of strontium and barium, respectively. The solid-state structure of the strontium salt **60** reveals a monomeric complex containing two ligands and a thf donor molecule. Both diiminophosphinate ligands act as

tripodal ligands co-ordinating the central metal ion via two pyridyl-N and one imino-N site. This is in contrast to **51**, where both imino-N sites chelate the metal in a highly symmetrical fashion and is surprising, as one would expect that alkaline earth metal centres do not benefit from π-acceptor properties of the 2-pyridyl groups, but instead prefer the electron rich diiminophosphinate chelate. A similar coordination mode is observed in the barium derivative **61**. This complex aggregates via 4,4′-bipyridyl molecules, which act as bridging units between barium ions to form a 1-D coordination polymer in the solid state. P–N bonds involving co-ordinating imino groups are on average only 4 pm longer than those of non-coordinating imino groups. The M–N(imino) bond lengths in **60** and **61** resemble those of symmetrical chelates in **53** and **54**. This suggests that the negative charge is still distributed over both imino groups, but polarised towards the co-ordinated N-centre. Some charge distribution from imino groups onto pyridyl rings is also considered. In comparison, P–N bond lengths in the protic precursor **59** differ by 12 pm (P–N 152.9, P–NH 164.9 pm). Dimethylzinc reacts with two equivalents of **59** under evolution of methane to form the homoleptic complex **62**. Both ligands co-ordinate via one pyridyl-N and one imino-N site to the metal centre. There is also a marked difference in P–N bond lengths (8 pm) observed in **62**, indicating high polarisation of negative charge within the N–P–N unit in the presence of Zn(II).

Reaction of **59** with BuLi did not give the deprotonated ligand but led, under loss of both silylimino functions, to lithium dipyridylphosphide **63**, which, however, can be directly obtained by deprotonation of dipyridylphosphine with BuLi [71]. Similarly, treatment of **59** with lithium bis(trimethylsilyl)amide does not lead to deprotonation but gives the lithium dipyridylphosphino silylamide complex **64**.

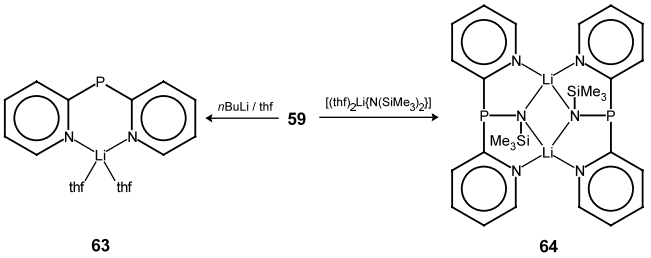

63 64

Reaction of bis(diphenylphosphino) amine with trimethylaluminium and treatment of the resulting dimethylaluminium diphosphinoamide dimer with one equivalent of trimethylsilylazide, gave the aluminium complex of an N-phosphino derivative of **II** (**65**). This complex was structurally characterised and accommo-

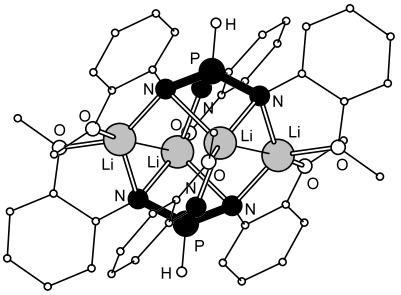

Fig. 7. Crystal structure of the dilithium triiminophosphonate (**67**).

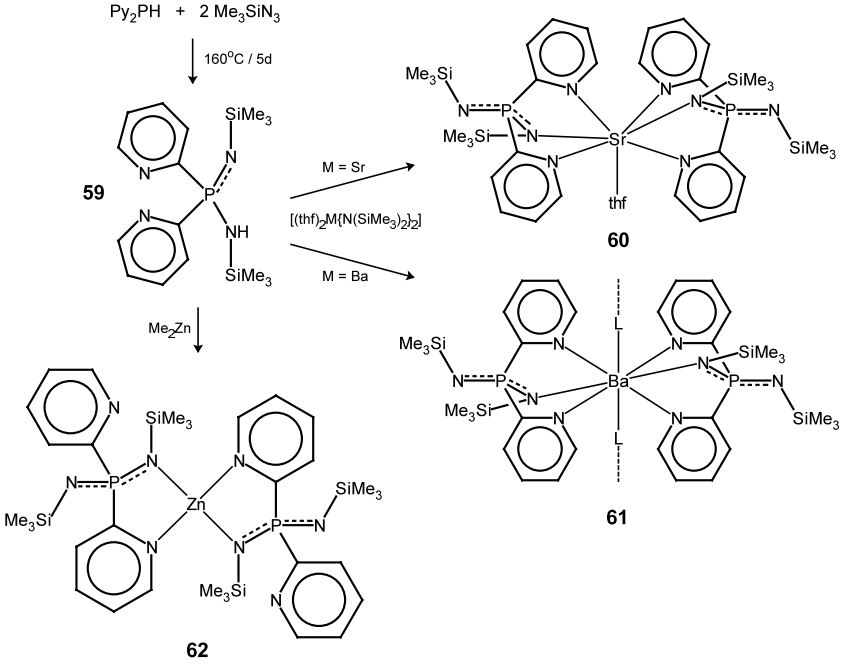

dates aluminium in a bidentate *N*,*N*′-chelation site. Me_2Al can be removed by reaction with potassium *tert*-butoxide to form the heterofunctional P,N-ligand **66** [72].

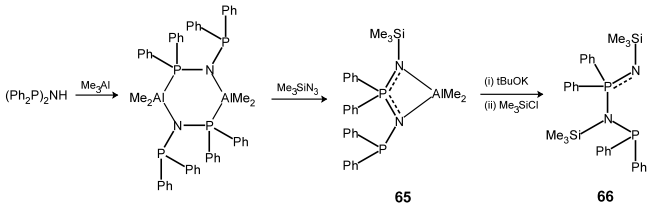

65 66

2.3. Triiminophosphonates, tetraiminophosphates and related systems

Compared with the thoroughly investigated diiminophosphinate ligand system **II**, very little has been studied on both **III** and **IV**, despite rich coordination potentials, as they are imino analogues of tridentate phosphonates and tetradentate phosphates, respectively. The only example of a dianionic triiminophosphonate **III**, which has been structurally determined, is the dimeric lithium complex **67** (Fig. 7) [73]. It has been generated by reaction of PCl_3 with 2-methoxyaniline in the presence of triethylamine and subsequent addition of *n*-BuLi. Corresponding to the oxo dianion HPO_3^{2-} the triimino analogue in **67** features a non-acidic P-bonded H atom, which is retained even after further addition of BuLi. The presence of the P–H unit is verified by the large ^1H to ^{31}P coupling constant ($^1J_{H-P} = 436$ Hz) and the appearance of the characteristic P–H stretching frequency in the IR spectrum at 2266 cm^{-1}. All imino-N atoms of the ligands as well as the methoxy groups are involved in coordination to metal ions. Two lithium ions reside in bidentate *N*,*N*′-chelates of one ligand plus a single interaction to the second ligand, whereas, the other two are singly co-ordinated to N-sites of each ligand. The P–N bonds are within the same range and on average 162 pm long. This is slightly longer than those observed in the lithium diiminophosphinate **43** and reflects the distribution of negative charge across three imino-N centres. In contrast, the corresponding arsenic derivative, which was generated using the same reaction conditions as above, contains the trianionic ligand $[(R'N)_3As]^{3-}$ [74].

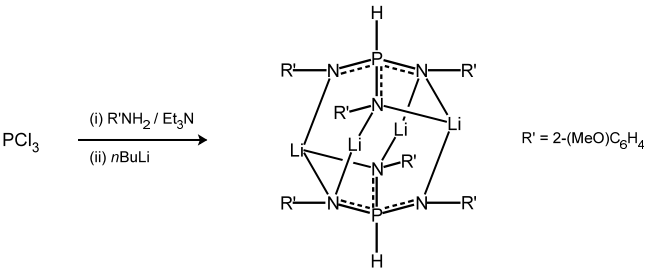

67

Bailey proposed the use of **III**, equipped with chiral substituents R′, as dianionic tripods for octahedral metal environments in asymmetric catalysis [75]. Reaction of tris(alkylamino) phenylphosphonium salts [76] with three equivalents of *n*-BuLi in thf yields the dianionic species (**68**) in solution. The presence of **68** was proved by methylation experiments: three-fold methylation of **68** occurs on reaction with MeI, but does not take place using the parent phosphonium salt $RP(NHR)_3Br$. However, treatment of **68** with $[(\eta\text{-p-cymene})RuCl_2]_2$ yielded $[(\eta\text{-p-cymene})Ru\{(i\text{-}PrN)_2P(Ph)(i\text{-}PrNH)][BPh_4]$ (**69**) after work-up. The cationic complex contains the mono-deprotonated ligand, which chelates the Ru centre via two imino-N sites. The intermediate complex containing the dianionic ligand proved to be highly moisture sensitive and was partially hydrolysed during standard inert gas work-up methods as indicated by a colour change from blue–green to purple. **69** is a rare example of a 16 electron Ru(II) complex containing an η6-bonded arene ligand, which reversibly binds CO. This illustrates the strong π-donating properties of the monoanionic ligand and the ability of poly(imino)phosphorus ligands to stabilise formally unsaturated species. Another example is the 16-electron Mn(I) complex $[(CO)_3Mn\{(Me_3SiN)_2P(OPh)N(SiMe_3)_2\}]$ which shows no tendency to co-ordinate CO to attain an 18-electron configuration [77]. Other complexes containing formally silylated monoanionic ligands **III**, which have been structurally described, include $[Cl_2Al\{(Me_3SiN)_2P(Ph)N(SiMe_3)_2\}]$ [78] and $\{PhZn\{(Me_3SiN)_2P(Ph)N(SiMe_3)_2\}]$ [79]. In both cases bidentate chelation patterns are observed.

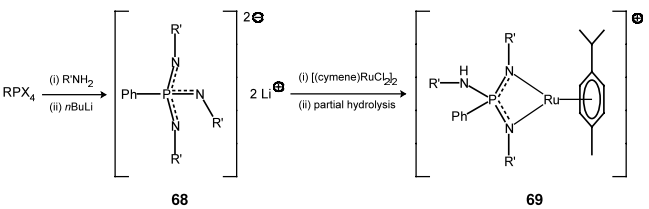

68 69

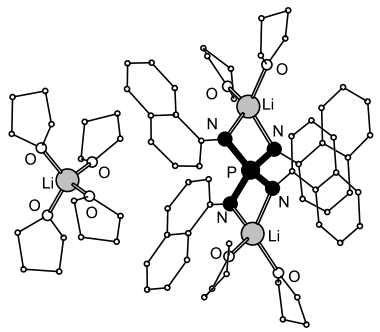

Fig. 8. Crystal structure of trilithium tetraiminophosphate (**70**).

Recently, an example of the tetraiminophosphate

anion **IV** was reported. The lithium complex (**70**) was recovered after reaction of diphosphorus tetraiodide with α-naphtylamine and subsequent addition of butyllithium [80]. X-ray structure determination revealed a solvent separated ion pair (Fig. 8). The complex anion consists of the trianionic ligand accommodating two lithium ions in two bidentate chelation sites. The cationic complex contains a lithium ion surrounded by four thf molecules. Both complex anion and cation show crystallographic D_2 symmetry. The PN_4 core of the ligand adopts a distorted tetrahedral geometry. Chelating N–P–N units have a narrow bond angle of 97.3°, whereas, angles of non-chelating N–P–N are wider (113.1 and 118.7°). The P–N bond length amounts to 164.5 pm and is slightly longer than in the triiminophosphonate. As expected, the P–N bond order decreases due to distribution of negative charge across four N-atoms. The mechanism of this reaction is somewhat unclear. However, it is known that hydrolysis of P_2I_4 under basic conditions leads to P–P cleavage and oxidation to form PO_4^{3-} ions amongst the formation of other products [81].

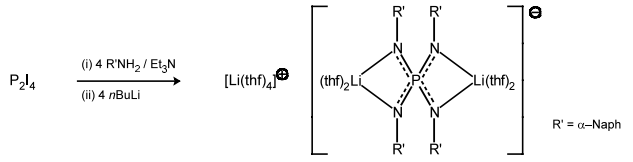

70

Preliminary studies show that tetraiminophosphates **IV** can also be synthesised in a more rational way by deprotonation of tetraaminophosphonium halides with organolithium reagents. Titration of $[P(NHR)_4]Cl$ with BuLi was followed by ^{31}P-NMR and showed a sequential deprotonation pattern similar to that of phosphoric acid, finally yielding the fully deprotonated tetraiminophosphate $[P(NR)_4]^{3-}$ [82].

The steric bulk of the imino groups facilitate the isolation of imino analogues of instable oxo derivatives. Monomeric metaphosphate PO_3^- (isovalence electronic to NO_3^-) is only stable in the gas phase and under matrix conditions and appears as an intermediate in several phosphorylation reactions. Niecke and co-workers have developed synthetic routes towards triiminometaphosphates $[P(NR')_3]^-$, which contain, in contrast to **IV**, trigonal planar PN_3 cores [83]. This facilitates π-type delocalisation across the central P-atom as *ipso*-C atoms of R′ are more or less within the plane of the central core. Two routes towards aminodi(imino)phosphorane **71** (= tris(imino) metaphosphoric acid) have been described (Scheme 3): (i) elimination of N_2 from dihydro tetraazaphosphole and (ii) treatment of chlorodi(imino)phosphorane with a primary lithium amide. Subsequent deprotonation leads to formation of lithium salts of $[P(NR')_3]^-$. X-ray structure analysis revealed that, depending on the steric bulk of R′, $L_nLi[P(NR')_3]$ (L = donor molecule) forms both contact (**72a**) and solvent separated (**72b**) ion pairs. In **72a** lithium is chelated within one N–P–N unit, which shows a rather acute N–P–N angle of only 88.4°, P–N bond lengths towards co-ordinating lithium atoms are on average 156 pm long with a tendency of the non-co-ordinated P–N bond to be only 2 pm shorter. In contrast, the free anion in the separated ion pair **72b** adopts crystallographic C_3 symmetry. P–N bonds are 156.5 pm long and N–P–N angles 119.9°. P–N bonds in both **72a** and **72b** are around 8 pm shorter than in **70** and reflect the increased multiple bond character around the three-co-ordinated P(V) centre.

In a previous attempt to generate imino analogous of monomeric metaphosphates bis(trimethylsilyl)aminobis(trimethylsilylimino)phosphorane (**73**) was reacted with carbonyl rhenium(I) halides. However, the initially formed complex **74** undergoes [2+2] cyclodimerisation forming complex **75** (amongst other products). The resulting dianionic ligand in **75** can be regarded as a condensed bis(triiminometaphosphate) [84].

In a more straightforward procedure, the parent diprotic acid of the dimerised ligand is obtained by

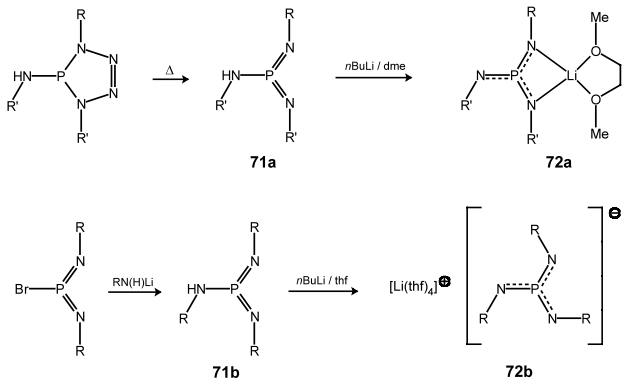

71a **72a** **71b** **72b**

Scheme 3.

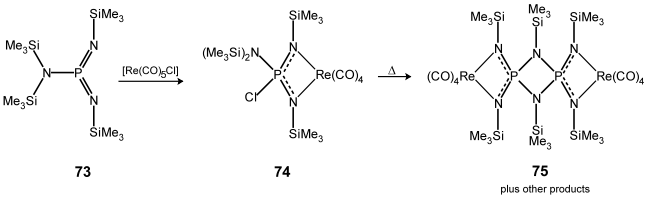

73 **74** **75**

double Staudinger reaction of **76** [85], which is easily prepared by treatment of PCl_3 with primary alkylamines. Reaction with trimethylaluminium gives the dinuclear species **78** [86].

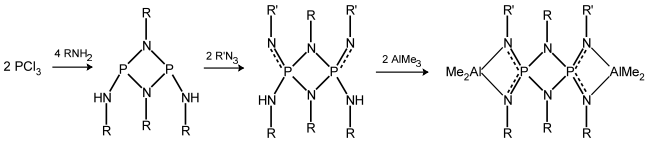

76 77 78

Also noteworthy, although, not within the scope of this review, is the diimino-P(III) ligand system $[P(NR)_2]^-$, which is the imino analogue of metaphosphite PO_2^- and is isovalence electronic to NO_2^-. Its lithium salt **79** is obtained by deprotonation of sterically bulky aminoiminophosphines **80**, which again are electronically related to metaphosphorous acid HPO_2 and nitrous acid HNO_2. Two types of lithium complexes have been obtained: (i) monomeric complex **79a** contains diethylether as donor solvent leading to a trigonal planar coordination around lithium and (ii) dimeric **79b** features two almost linearly co-ordinated lithium ions. P–N bond lengths in **79a** and **79b** are on average 159 pm long [87]. The low coordination numbers of metal ions in both complexes is being accomplished by the steric demand of substituents R.

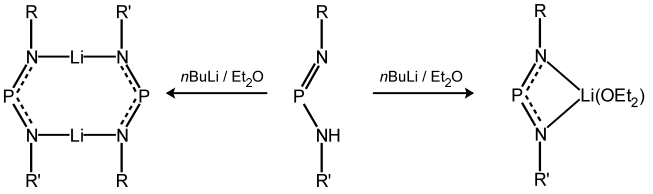

79b 80 79a

In a similar manner as **72**, **80** undergoes [2+2] cycloaddition on heating to form derivatives of the condensed diacid **76** [88]. In the presence of appropriate metal bases **76** is doubly deprotonated. The resulting dianionic ligand system has been applied in various metal complexes [89].

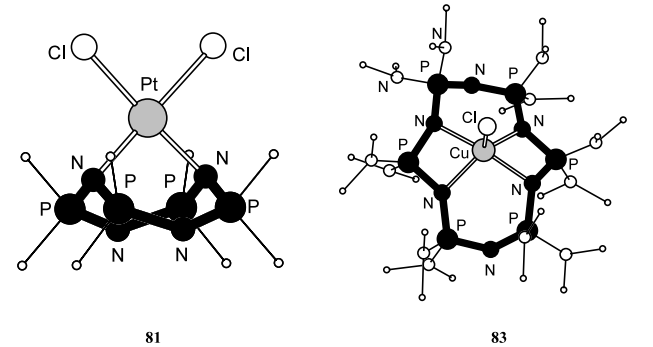

81 83

Fig. 9. Crystal structures of cyclophosphazene metal complexes.

3. Aza-P(V) ligands

3.1. Phosphazenes

The most prominent class of compounds featuring aza bridges between P(V) centres are cyclic and polymeric phosphazenes $(R_2P–N)_n$. The P–N bond in phosphazenes exhibits multiple bond character, which is slightly lower than in iminophosphoranes (**I**) as indicated by slightly longer P–N bond lengths and lower P–N stretching frequencies ($\sim$1200 cm^{-1}) [90]. The P–N backbone in phosphazenes is isoelectronic to the Si–O backbone in siloxanes $(R_2Si–O)_n$. It is kinetically more inert than the Si–O backbone due to the higher bond order, which makes the P(V) centre less prone to nucleophilic attack. The high thermal and chemical stability of the phosphazene backbone has led to special applications of the polymer, such as usage in fire retardants, coating agents for electrical components and fuel pipes [91].

Cyclotriphosphazenes (**V**) and cyclotetraphosphazenes have been studied extensively [92]. Straightforward substitution reactions, starting from the halo derivatives $(X_2P=N–)_n$ (X = F, Cl) allow the introduction of wide range of substituents R [93]. The N-ring atom is able to interact with metal centres via the sp^2 hybridised lone pair. Electron donating R groups enhance the basicity of N-ring sites. Spectroscopic data show, that phosphazenes are predominantly σ-donors with only minor π-acceptor properties [94]. The coordination chemistry of phosphazenes has been reviewed comprehensively [95]. Here, we briefly illustrate the coordination ability of the ring nitrogen atom.

The octacyclic cyclotetraphosphazene is highly puckered and allows di-hapto coordination as observed in Pt(II) complexes **81** which feature square planar metal environments [96]. P–N bonds in **81** involved in metal coordination are on average 6 pm longer than those not associated with M–N interactions. N(*endo*) positions of phosphazenes are moderately basic and bind protons at low pH. In Complex **82** the eight-membered phosphazene ring binds one proton and co-ordinates to a $CuCl_3$ unit at opposite N(*endo*) centres [97]. P–N bonds in **82** involving the protonated N(*endo*) atom are quite long (167 pm) compared with those of the Cu-co-ordinating

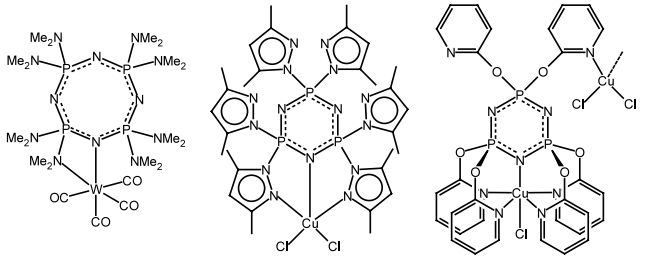

Scheme 4.

N-atom (163 pm). Higher ring homologues, in particular derivatives of cyclohexaphosphazenes **83** provide six N-donor sites, of which four co-ordinate the encapsulated metal ion [98]. The coordination pattern of these macrocyclic ligands resembles that of crown ethers. P–N bonds are elongated on M–N interactions. Crystal structures of **81** and **83** are displayed in Fig. 9.

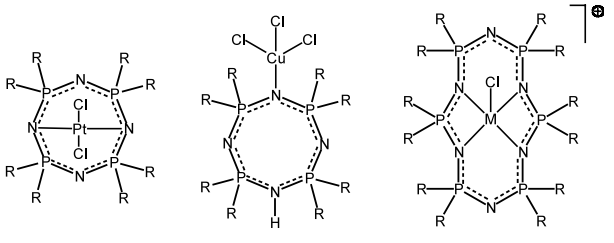

81 **82** **83**

A number of phosphazene ligands have been reported, which provide additional coordination sites at the *exo*-cyclic substituents. These include amino [99,100] pyrazol-1-yl [101], 2-pyridinoxy [102] and 2-pyridilamino functions [103]. These neutral ligands offer multidentate co-ordination cavities for one or two metal ions. Examples of metal complexes of such ligands are illustrated in Scheme 4.

Some metal derivates of phosphazene polymers have been reported. This include the polymeric analogue of Pt(II) complex **81**, which shows anticancer activity [104]. Molecular cyclophosphazenes such as **81** act as model compounds for the analogous polymer, as structural parameters and synthetic routes are investigated more conveniently using small molecular species [105]. Polyphosphazenes carrying linear or branched polyether side chains dissolve lithium salts. The resulting polymeric electrolyte shows low glass-transition temperature and high electric conductivity, exceeding that of the widely used poly(ethylene oxide) [106], which promise application in fuel cells such as lithium batteries. Another recent development is the use of poly(methylphenylphosphazenes) as a stabilising medium in the synthesis of gold nanoparticels. The stabilisation is believed to result from the interaction of gold with the basic nitrogen centres in the polyphosphazene backbone [107].

Like the iminophosphorane unit, the phosphazene ring has acceptor properties and, correspondingly, α-H atoms at alkyl substituents show acidic behaviour in the presence of organolithium reagents. Methyl derivatives of cyclotri- and cyclotetraphosphazenes, are deprotonated by alkyllithiums as shown by the subsequent introduction of electrophiles. The study shows that only one methyl group per phosphorus-atom in both $Me_6P_3N_3$ and $Me_8P_4N_4$ is deprotonated [108]. It is assumed that in the intermediate lithiated species **84** lithium resides in C,N-chelation sites, probably similar to the coordination mode of α-deprotonated iminophosphoranes (**9**). Likewise, methyl groups in poly(methylphenylphosphazene) are deprotonated by *n*-BuLi [109]. Subsequent treatment with electrophiles facilitates modification of phosphazene side chains.

The α-deprotonation reaction of dimethylphosphazenes $[-(Me_2)P{=}N-]_n$, is remarkable if compared with backbone cleavage of isoelectronic siloxanes $[-(Me_2)Si-O-]$ in the presence of strong nucleophiles [110], and it nicely demonstrates the kinetic inertness of the phosphazene backbone structure, which is retained even under most severe reaction conditions.

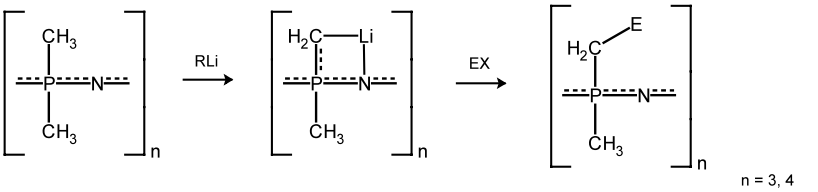

84

R = Me, *n*Bu

EX = MeI, Br_2, I_2, Me_3SiCl, Me_3SnCl_2, $PhCO_2Et$

4. Imino–aza-P(V)-ligands

4.1. Linear diiminophosphazenates

Linear diiminophosphazenates consist of an open chain phosphazene backbone equipped with terminal imino groups, =NR′, at both ends and are monoanions of the general formula $[R'N-(R_2P-N)_n-R_2P-NR']^-$. To date, only the short chain species **VI** ($n = 1$) has been reported, although, longer chain systems ($n > 1$) might be accessible using standard synthetic methods. The synthetic route to build-up **VI** proceeds via 'bezman-salt' (**85**), which is obtained by reaction of trihalo

phosphorane with excess ammonia [111]. Subsequent deprotonation and stepwise silylation gives **86** and **87**, respectively [112]. Deprotonation of **87** with appropriate metal bases gives complexes of the monoanionic ligand **VI**.

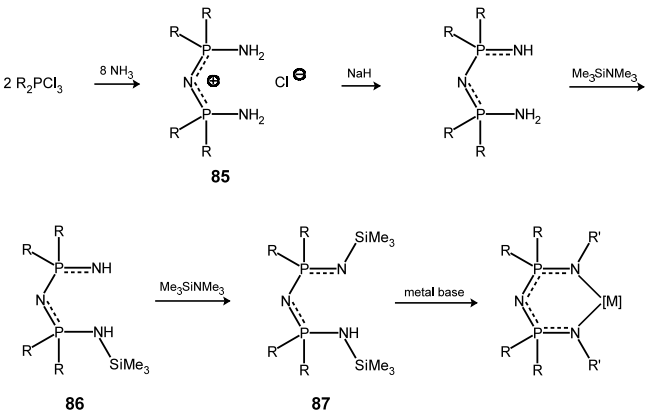

A number of main group metal complexes of **VI** have been described. Solid-state structures show that both imino and aza N-functions act as coordination sites in alkali and alkaline earth metal complexes. The dimeric lithium complex $[Li_2\{N(Ph_2PNSiMe_3)_2\}_2]$ (**88**) was obtained from deprotonation of **87** (R = Ph) with *n*-BuLi [113]. Each lithium ion is four-co-ordinated by N(aza)–N(imino) chelates of both ligands; the N(aza) atoms bridging both lithium atoms (Fig. 10). Structural data reveal that P–N(imino) bonds are shorter (average 157 pm) than P–N(aza) bonds (average 162) suggesting the polarisation of negative charge toward the central N(aza) atom [114]. Strangely, N(imino)–Li contacts are considerably shorter than N(aza)–Li contacts (average 25 pm). One explanation for this behaviour could be that both metal ions are perfectly encapsulated by two ligands, which bring them into close contact (Li···Li 2.789 pm). Hence, repulsion between metal ions, leads to distorted coordination geometries by pushing the metal

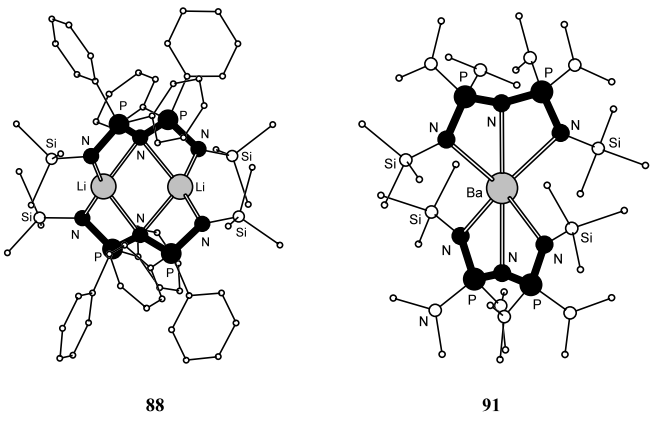

Fig. 10. Crystal structures of diiminophosphazenates of lithium and barium.

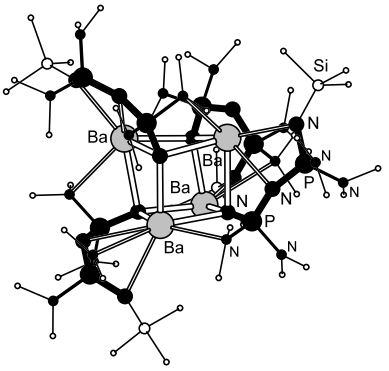

Fig. 11. Crystal structure of tetrameric barium complex **94**.

ions away from the central coordination sites of the ligand. Sodium and potassium derivatives were prepared by reaction of the **87** (R = NMe_2) with metal hydrides [115]. The sodium complex $[Na_2\{N((Me_2N)_2PNSiMe_3)_2\}_2]$ (**89**) is dimeric in the solid state. Sodium ions are co-ordinated to three N-functions of one ligand and one N(imino) atom of the other ligand. The potassium complex exists as a coordination polymer in the solid state involving not only aza-N and imino-N centres, but also dimethylamino side groups in metal coordination. The tendency to exhibit short P–N(imino) and longer P–N(aza) bond lengths is still apparent in both Na and K derivatives, but is less pronounced than in **88**. Calcium [115] and barium [116] derivatives ($[Ca\{N((Me_2N)_2PNSiMe_3)_2\}_2]$ (**90**), $[Ba\{N((Me_2N)_2PNSiMe_3)_2\}_2]$ (**91**) (Fig. 10)) are synthesised by the reaction of **87** (R = NMe_2) with $M\{(N(SiMe_3)_2\}_2$. Both are structurally equivalent: metal ions show distorted octahedral coordination spheres and are effectively shielded by the two bulky tridentate ligands. In contrast to dinuclear **88**, mononuclear alkaline earth metal complexes show short M–N(aza) and slightly longer M–N(imino) bonds. P–N(imino) bond lengths (average 157 pm) are very similar to P–N(aza) bond lengths

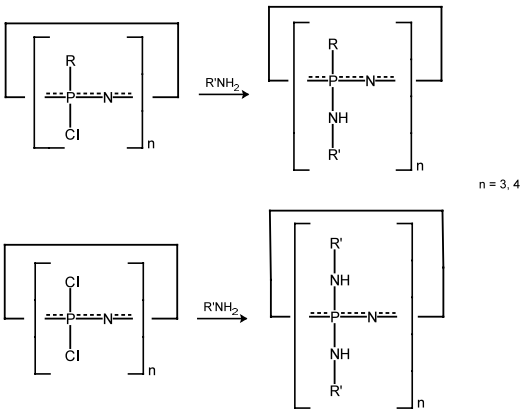

Scheme 5.

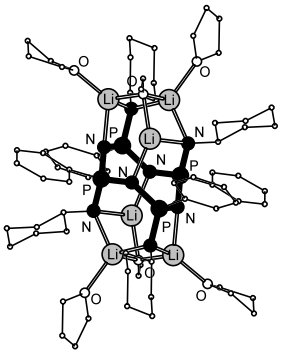

Fig. 12. Crystal structure of $[(thf)_6Li_6\beta\text{-}trans\text{-}\{(Ph)(CyNH)P\}_4N_4(CH_2{=}CHO)_2]$ (**96a**).

(average 158 pm) indicating equal charge distribution across all N-centres in the diiminophosphazenate backbone. **90** and **91** are rare examples of monomeric homoleptic complexes of heavy alkaline earth metals. Sol–gels of **91** give $Ba(OH)_2 \cdot x(H_2O)$, a potential precursor for the synthesis of complex Ba-oxides. Reactions of MMe_3 (M = Al, Ga, In) with **87** (R = Ph) yield monomeric complexes $[Me_2M\{N(Ph_2PNSiMe_3)_2\}]$ (**92**) containing six-membered metalacycles [113]. Similarly $Zn\{N(SiMe_3)_2\}_2$ reacts with **87** (R = NMe_2) to form the six-membered ring structure $[\{(Me_3Si)_2N\}Zn\{N((Me_2N)_2PNSiMe_3)_2\}]$ (**93**) [117]. Exclusively, N(imino)-functions are involved in metal coordination in both **92** and **93**. In contrast to **88**, P–N(imino) distances are longer than P–N(aza) distances (3 pm in the Zn and 8 pm in the Al structure), suggesting polarisation of electron density towards co-ordinating N(imino) functions due to the stronger Lewis-acidity of Al(III) and Zn(II)centres.

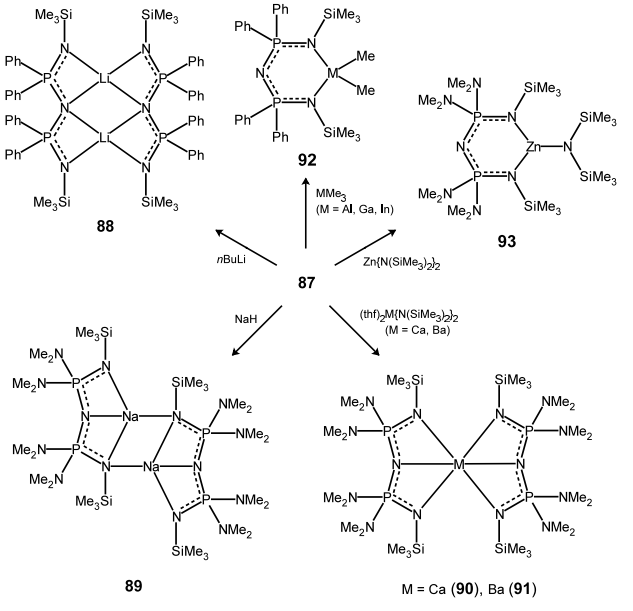

A highly aggregated complex has been obtained from the reaction of the diprotic monosilyl precursor **86** with one equivalent of $[(thf)_2Ba\{N(SiMe_3)_2\}_2]$ [116]. The core of the tetrameric barium complex $[Ba_4\{N(Me_2N)_2PN(Me_2N)_2PNSiMe_3\}_4]$ (**94**) consists of a Ba_4N_4 heterocubane structure (Fig. 11). All four barium ions have unique environments of coordination numbers of five, six and seven. In contrast to the mononuclear barium complex **91**, where only imino and aza nitrogen atoms are involved in metal coordination, amino N-atoms of side chains act as additional donor centres in **94**.

4.2. Cyclic poly(imino)phosphazenates

Cyclic poly(amino)phosphazenes are deprotonated by strong metal bases, yielding multianionic poly(imino)cyclophosphazenates **VII** and **VIII**. The multiprotic poly(amino)phosphazene precursors are synthesised by reaction of chlorophosphazenes with primary amines in the presence of an auxiliary base [118]. A wide variety of primary amines can be used in this procedure. Depending on the number of available chloro positions at P, each phosphorus atom can take up either one or two protic RNH groups as outlined in Scheme 5.

Cyclic non-geminal *P*-chloro-*P*-organophosphazene precursors $[-(Cl)(R)P{=}N-]_n$ ($n = 3, 4$) exist as different stereoisomers, which usually retain their configuration upon the aminolysis reaction. Thus, treatment of β-*trans*-$[\{(Ph)(Cl)P\}_4N_4]$ with cyclohexylamine gives tetraprotic β-*trans*-$[\{(Ph)(CyNH)P\}_4N_4]$ (**95**). Reaction of the latter with *n*-BuLi in toluene yields the tetralithiated tetraiminocyclotetraphosphazenate **96** [119]. Reaction of **95** with excess *n*-BuLi in thf gave single crystals suitable for X-ray structure determination (Fig. 12). The structure of the hexalithium complex **96a** contains, in addition to the tetraanionic ligand, two enolate anions and four molecules of thf. Enolate formation occurred on degradation of thf by excess *n*-BuLi.

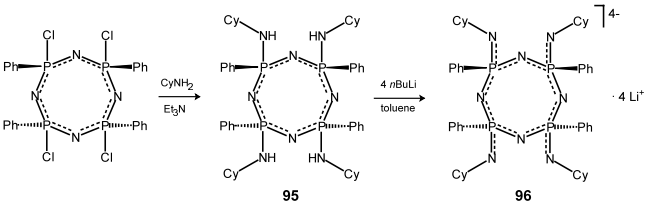

96a is monomeric in the solid state. The tetraanionic ligand exhibits two separated coordination sites forming concave shaped cavities. Both act in a tetradentate fashion involving all eight *endo* and *exo*-cyclic nitrogen atoms. Each cavity contains a triangular arrangement of lithium ions capped by the O-donor function of an enolate ion. *Exo*-cyclic and *endo*-cyclic P–N bonds are of equal length (on average 162 and 163 pm, respectively). This is in contrast to neutral β-*trans*-$[\{(Ph)(Me_2N)P\}_4N_4]$, where *exo*-cyclic bonds are considerably longer (average 168 pm) than *endo*-cyclic bonds (average 160 pm) [120]. This indicates that in

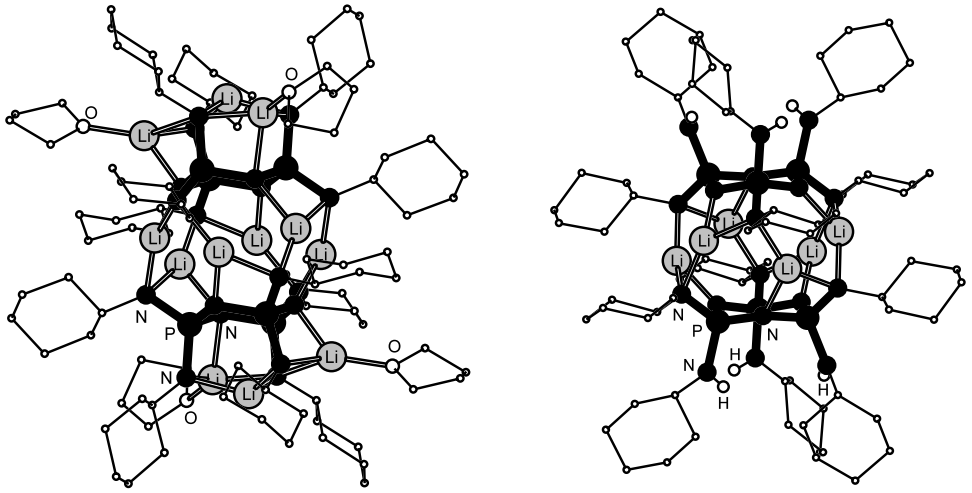

Fig. 13. Crystal structure of $[(thf)_4Li_{12}\{(CyN)_6P_3N_3\}_2]$ (**98a**) and $[Li_6\{(CyN)_3(CyNH)_3P_3N_3\}]$ (**99a**).

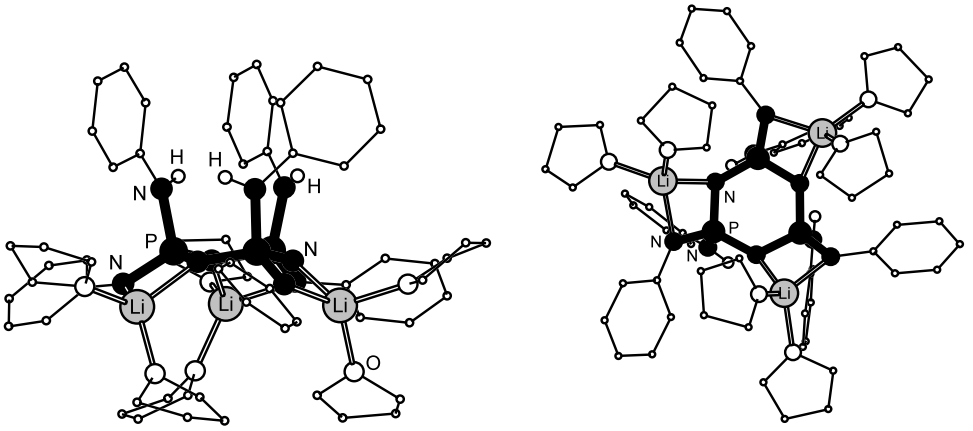

Fig. 14. Two views of the crystal structure of $[(thf)_6Li_3[(PhNH)_3(PhN)_3P_3N_3]$ (**99b**).

tetraanions, **VII**, the negative charge of the *exo*-cyclic N-atoms is partly transferred into the ring, which increases the bond order in the *exo*-cyclic P–N bonds and in return reduces the bond order in the ring.

Reactions of hexachlorocyclotriphosphazene and octachlorocyclotetraphosphazene with excess primary amine yield fully substituted amino derivatives $(RNH)_6P_3N_3$ (**97**) and $(RNH)_8P_4N_4$, respectively (see Scheme 5). $(CyNH)_6P_3N_3$ (**97a**) reacts as a hexaprotic acid with six equivalents of *n*-BuLi in thf. The solid-state structure of the resulting hexalithiated species **98a** exists as a dimer containing two hexaanionic ligands **VIII** and 12 lithium ions (Fig. 13) [121]. Six lithium ions are 'sandwiched' between the ligands and occupy bidentate N(*exo*)–P–N(*endo*) chelation sites. The remaining lithium ions are accommodated at the opposite sites of both ligands. The central P_3N_3 ring systems of both ligands are highly puckered exhibiting a chair conformation, which is in contrast to planar conformation of neutral cyclotriphosphazenes. P–N bond lengths throughout the P_3N_9 core are very similar (average P–N(*endo*) 166, P–N(*exo*/equatorial) 163 and P–N(*exo*/axial 164 pm). This suggest equal bond orders at *exo*- and *endo*-cyclic P–N bonds and equal distribution of negative charge over N(*exo*) and N(*endo*) atoms. $[(CyN)_6P_3N_3]^{6-}$ ions in **98a** are isoelectronic to cyclotrisilicate ions $[Si_3O_9]^{6-}$, but in addition equipped with cyclohexyl groups, which provide a lipophilic ligand surface and thus facilitate solubility in non-polar solvents.

Deprotonation pathways between $(RNH)_6P_3N_3$ and $[(RN)_6P_3N_3]^{6-}$ (R = Cy, Ph) using *n*-BuLi were monitored by ^{31}P-NMR [122]. The phenyl derivative gives exclusively the trianionic species $[(PhNH)_3(PhN)_3P_3N_3]^{3-}$ (**99b**) after addition of three equivalents of *n*-BuLi. In contrast, the cyclohexyl derivative did not show the appearance of a distinct species until addition of six equivalents *n*-BuLi. However, protolysis of **98a** with three equivalents of *n*-butanol yields trianionic $[(CyNH)_3(CyN)_3P_3N_3]^{3-}$ (**99a**) as the sole product.

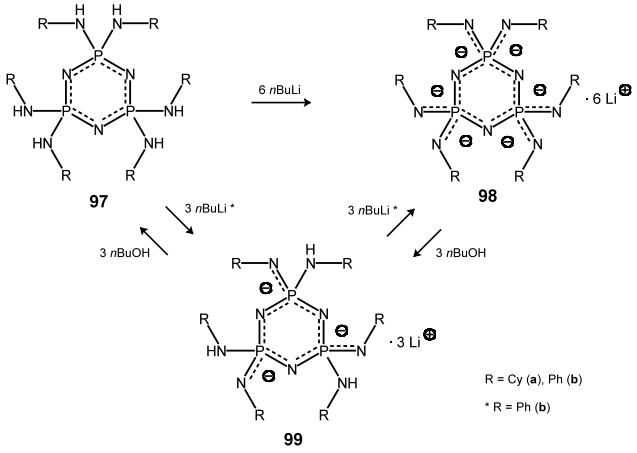

Crystal structures of both trianionic derivatives (R = Cy (**99a**, Fig. 13), Ph (**99b**, Fig. 14)) have been determined. Both contain puckered P_3N_6 rings of chair conformation. The deprotonation occurred stereospecifically in non-geminal *cis*-fashion at equatorial positions. **99a** forms a dimer in the solid-state. The hexanuclear lithium arrangement corresponds to the central cage structure in **98a**. On the other hand, **99b** is monomeric, but shows a similar coordination pattern as **99a** as three lithium ions occupy bidentate N(*exo*)–P–N(*endo*) chelation sites. In addition, two thf molecules co-ordinate each lithium ion. P–N distances of axial bonds involving the non-deprotonated amino functions are 5–10 pm longer than equatorial and *endo*-cyclic bonds indicating charge delocalisation across the latter two.

Comparison of structural and spectroscopic data of neutral hexaprotic $(CyNH)_6P_3N_3$ (**97a**), trianionic $[(CyNH)_3(RN)_3P_3N_3]^{3-}$ (**99a**) and hexaanionic $[(CyN)_6P_3N_3]^{6-}$ (**98a**) reveal an interesting tendency: as the ligand charge increases, the bond order within the ring decreases as a result of enhanced charge transfer from deprotonated *exo*-cyclic onto *endo*-cyclic N-centres. This is indicated by a considerable red shift of the P–N-ring stretching frequency from **97a** (1194 cm^{-1}), **99a** (1095 cm^{-1}) to **98a** (1031 cm^{-1}) accompanied by an increase in P–N(*endo*) bond lengths from 1.598 (**97a**), 1.635 (**99a**) to 1.660 Å (**98a**) and narrowing of N–P–N(*endo*) angles [116.3° (**97a**)-112.3° (**99a**)-109.7° (**98a**)]. As *endo*-cyclic N–P–N angles become more and more acute, ring puckering becomes more distinct, as shown by increasing torsion angles within the central P_3N_3-ring: **97a** (average 3.6° ~planar), **99a** (average 33.2°) and **98a** (average 43.7°).

The successive deprotonation pattern involving neutral **97**, trianionic **99** and hexaanionic **98** resembles that of mononuclear polyprotic oxy acids. It is, however, shifted towards the far basic region of the acidity scale, and both kinetic control and ion pairing seem to play a significant role. The phosphazene backbone of these systems withstands nucleophilic attack by strong bases such as butyllithium, even if used in excess. In contrast, condensed oxoacids are prone to backbone cleavage in the presence of strong bases and lack corresponding acid–base reactions and oxoanions isoelectronic to **99** such as $[H_3Si_3O_9]^{3-}$ are unknown.

Aluminium derivatives were prepared by treatment of **97a** with excess trimethylaluminium. Metalation takes place sequentially under selective occupation of distinct coordination sites. The reaction proceeds in toluene at r.t. to give exclusively the trinuclear aluminium complex $[(Me_2Al)_3\{(CyN)_3(CyNH)_3P_3N_3\}]$ (**100**), which contains the triply deprotonated ligand [123]. Further deprotonation occurs as the mixture is refluxed yielding the pentanuclear aluminium complex $[(Me_2Al)_4(MeAl)\{(CyN)_6P_3N_3\}]$ (**101**). Both species were structurally characterised (Fig. 15), the latter as the thf adduct $[(Me_2Al)_4(thfMeAl)\{(CyN)_6P_3N_3\}]$ (**101a**) [124]. Me_2Al units in **100** are accommodated at 'inner' N(*endo*)–P–N(*exo*) chelates around the central phosphazenate ring. In contrast to **99**, triple deprotonation occurred in non-geminal *trans* fashion. **101a** hosts the additional two Al

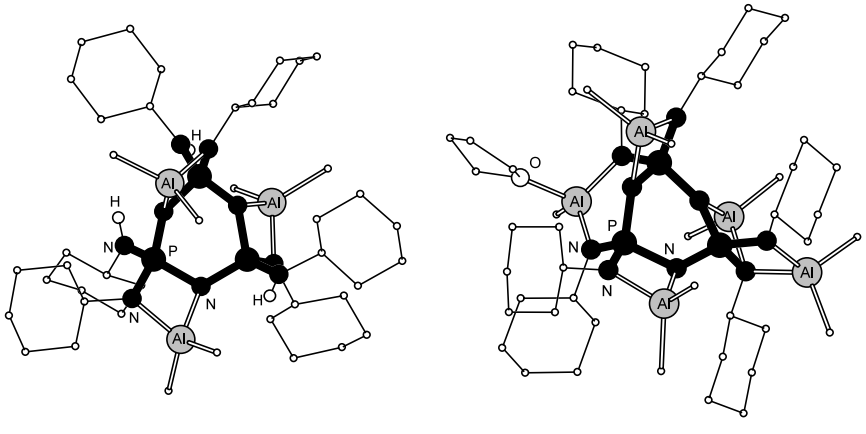

Fig. 15. Crystal structures of tri-and pentanuclear aluminium complexes.

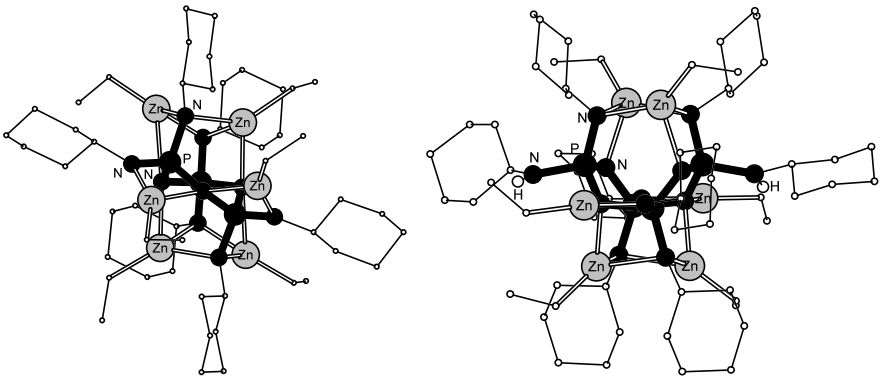

Fig. 16. Crystal structures of hexanuclear zinc complexes **102** and **103**.

centres at the more remote 'outer' sites: the Me_2Al unit occupies an N(*exo*)–P–N(*exo*) chelate, while the (thf)MeAl unit forms a six membered metalocycle involving bidentate N(*exo*)–P–N(*endo*)–P–N(*exo*) chelate.

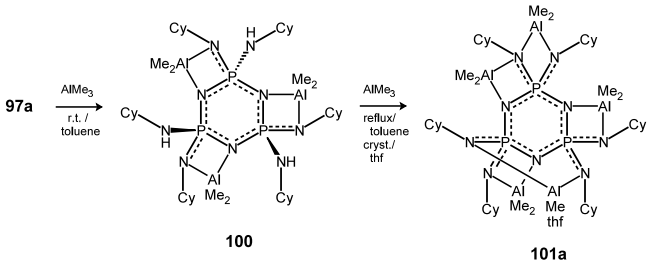

100 **101a**

In order to obtain multinuclear zinc complexes, $(CyNH)_6P_3N_3$ as well as $(CyNH)_8P_4N_4$ were refluxed with excess diethyl zinc in toluene. In both cases, six-fold deprotonation occurred to give $[(EtZn)_6\{(CyN)_6P_3N_3\}]$ (**102**) and $[(EtZn)_6\{(CyN)_6(CyNH)_2P_4N_4$ (**103**) (Fig. 16) [124]. $(CyNH)_8P_4N_4$ is not deprotonated completely even after prolonged heating of the reaction mixture. Both complexes show similar coordination pattern, as four Zn atoms occupy tripodal sites, and two zinc atom are chelated by bidentate N(*exo*)–P–N(*endo*) sites. The six-membered phosphazenate ring in **102** is highly puckered and adopts a twist conformation. An interesting feature of **102** is the side-on coordination of the central phosphazene ring towards four zinc atoms, giving almost linear Zn–N(*endo*)–Zn arrangements (average 157°). However, these interactions are most likely a consequence of the high metal loading and not due to any tendency of zinc to form π-interactions with the phosphazene ring.

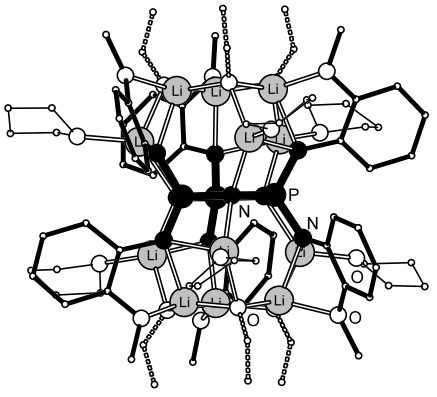

Fig. 17. Crystal structure of $[(thf)_6Li_{12}\mathbf{A}(CH_2{=}CHO)_6]$ (**105**). The ligand $\mathbf{A}^{6-}$ is drawn in black and the enolate ions dashed.

Imino phosphazenate anions show diverse coordination modes by employing both N(imino) and N(aza) functions to form a variety of bidentate and tridentate coordination sites. Scheme 6 lists the so far observed coordination modes of hexaanionic ligand system **VIII**. It is interesting to note that in all structurally characterised phosphazenate complexes there is no metal coordination of non-deprotonated amino substituents observed, despite high ligand charge and extensive metal loading. This suggests that non-deprotonated RNH functions have no or only very poor donor abilities.

The high ligand charge and the large number of N-donor sites facilitate high metal loading per ligand molecule. For example, **102** and **103** contain the largest number of zinc centres, which are accommodated within a single ligand. However, the metal loading capacity can

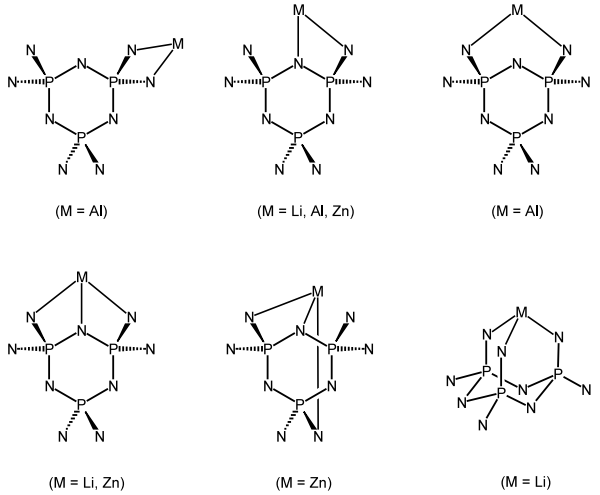

Scheme 6.

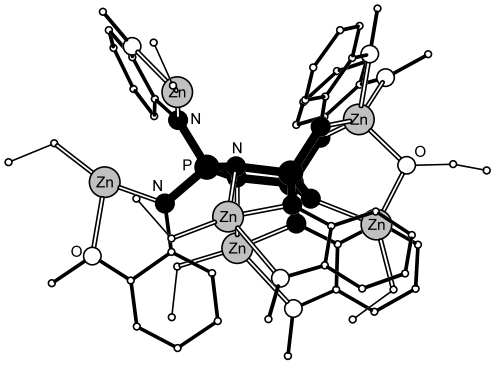

Fig. 18. Crystal structure of hexanuclear zinc complex $[(EtZn)_5Zn(EtO)\mathbf{A}]$ (**106**).

be maximised further by introduction of additional donor sites into the ligand periphery: $H_6\mathbf{A}$ ($\mathbf{A} = [\{2\text{-}(MeO)C_6H_2N\}_6P_3N_3]^{6-}$) (**104**) carries six 2-(methoxy) phenyl groups and reacts with 12 equivalents of *n*-BuLi in thf to give the monomeric dodecanuclear lithium complex $[(thf)_6Li_{12}\mathbf{A}(CH_2{=}CHO)_6]$ (**105**) (Fig. 17). The complex also contains six enolate anions resulting from degradation of thf [125]. The hexaanionic pentadecadentate phosphazenate ligand $\mathbf{A}^{6-}$ accommodates 12 lithium ions in bidentate chelation sites. Six lithium ions reside at 'inner' N(*exo*)–P–N(*endo*) sites, while the other six lithium ions occupy the 'outer' N(*exo*),O-chelates of the anisidyl side groups. ^{31}P-NMR monitoring of above reaction reveals that once the ligand is triply deprotonated, both further deprotonation and thf degradation occur simultaneously, as the highly charged ligand acts as a Li^+-sponge dragging excess butyllithium into the ligand sphere, which accelerates degradation of thf. ^{7}Li-NMR show that lithium ions are tightly bound to the ligand and do not fluctuate within the complex.

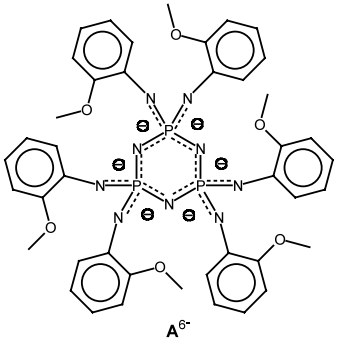

$H_6\mathbf{A}$ + 12 nBuLi + 12 thf ⟶ $(thf)_6Li_{12}A(CH_2{=}CHO)_6$ + 12 C_4H_{10} + 6 C_2H_4

104 **105**

Two multinuclear zinc complexes have been obtained very recently, which nicely illustrate the flexibility of the multianionic multi donor ligand $\mathbf{A}^{6-}$ [126]. Reaction of **104** with excess diethylzinc yielded the hexanuclear zinc complex $[(EtZn)_5Zn(EtO)\mathbf{A}]$ (**106**) (Fig. 18). The formation of ethoxide stems from insertion of oxygen into one Zn–C bond. Four ethylzinc moieties are chelated within the 'outer' N(*exo*),O-chelates of *ortho*-anisidyl chelates. Two of these four EtZn units form additionally loose interactions to the central phosphazene ring. The fifth ethylzinc unit is co-ordinated to an N(*endo*) atom and the ethoxy ligand, whereas, the sixth zinc atom does not carry an ethyl group and is pentacoordinated by two N(*exo*) atoms, two methoxy groups of anisidyl substituents and the ethoxy ligand.

The complex $[Zn_4(H_2\mathbf{A})_2]$ (**107**) was isolated upon partial protolysis of **106** and shows a quite different coordination pattern. It contains two $H_2\mathbf{A}^{4-}$ tetraanions, which encapsulate the tetranuclear zinc arrangement (Fig. 19). In contrast to partially deprotonated **99** and **100**, the two protonated N(*exo*) functions are attached to the same phosphorus atom. None of the protonated anisidyl groups take part in metal coordination. However, the four deprotonated substituents as well as their central N(*endo*) functions form a nonadentate coordination surface. Upon dimerisation both ligands interlock to form a capsule, large enough to host four zinc(II) centres. Two zinc ions are penta- and the other two hexa-coordinated involving 'inner' N(*endo*) and N(*exo*) functions and 'outer' methoxy groups. The ligand is highly flexible and can adopt itself to a particular metal environment, as inner rotation around all P–N(*exo*) and N(*exo*)–C(*ipso*) bonds facilitates a large number of ligand conformations.

4.3. Poly(imino)phosphazenate cages and 3D-networks

Molecular complexes containing cage type multianions such as **IX** have not been prepared yet. However, high temperature reactions of phosphorus nitrides with alkali metal nitrides and amides gave solid-state materials, which contain multianionic species related to **IX**. $RbNH_2$ reacts with P_3N_5 (molar ratio 6:1) at 400 °C within 5 days to yield $Rb_8[P_4N_6(NH)_4](NH_2)_2$ (**108**). It contains the hexaanion $[P_4N_6(NH)_4]^{6-}$ comprising an adamantane P_4N_6 core structure equipped with four terminal imino functions at each phosphorus atom and

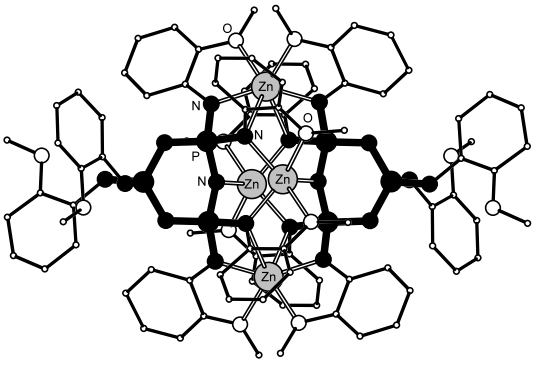

Fig. 19. Crystal structure of tetranuclear zinc complex $[(Zn_4(H_2\mathbf{A})_2]$ (**107**).

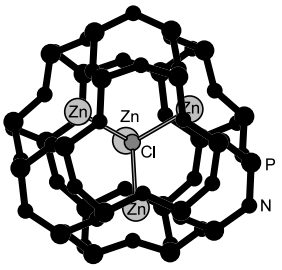

Fig. 20. β-Cages $[P_{12}N_{24}]$ accommodating $[Zn_4Cl]^{7+}$ arrangements in **109**.

is isoelectronic with P_4O_{10} [127]. All ten nitrogen atoms co-ordinate to rubidium ions. The P–N(aza) bonds are longer (average 165.6 pm) than the P–N(imino) bonds (160.8 pm). This suggests that the P–N bonds within the adamantane cage have lower bond order and that the divalent aza nitrogen centres ought to be strongly basic.

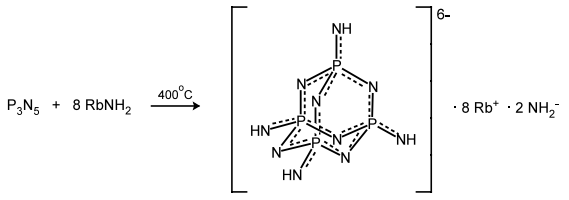

108

A very interesting class of compounds are lithium phosphorus nitrides, which are obtained from solid-state reactions of lithium nitride Li_3N with phosphorus nitride P_3N_5 at high temperatures (600–800 °C) [128]. Depending on the molar ratio of these precursors, ceramic type materials Li_7PN_4, $Li_{12}P_3N_9$, $Li_{10}P_4N_{10}$ and $LiPN_2$ were prepared. These contain anions, which resemble P–N ligand frameworks discussed in this account. PN_4^{7-} is electronically related to **IV**, $P_3N_9^{12-}$ to **VIII** and $P_4N_{10}^{10-}$ to **IX**. $LiPN_2$ contains the anionic 3-D framework $\{[PN_2]^-\}_\infty$, which is isoelectronic to SiO_2 and topologically equivalent to β-crystobalite [129]. This compound is interesting in this context as its anionic moiety is entirely composed of tetravalent phosphonium (P) and divalent amide (N) units, the basic building blocks of discussed imino–aza-P(V) ligands. Likewise, $Zn_7[P_{12}N_{24}]Cl_2$ (**109**) is based on an anionic framework of composition $\{[PN_2]^-\}_\infty$ [130]. It represents a phosphazenate analogue of a zeolite, as it contains β-cages $[P_{12}N_{24}]$ and forms a sodalite type structure (Fig. 20).

5. Summary

A wide variety of imino–aza phosphorus(V) ligand systems has been developed over recent years. They have been utilised as sterically demanding, electron rich donor ligands in various areas of coordination chemistry. This includes stabilisation of low coordination numbers, unusual oxidation states and bonding modes, as well as ligands for homogeneous catalysis. N(imino)-silyl derivatives of **I** [131], **II** and **VI** [132] have served as starting compounds for the synthesis of metala-P–N-heterocycles and cage complexes.

The other driving force behind this research has been the quest for imino analogues of well-known oxo anions, such as phosphates, phosphonates, silicates etc. as well as of unstable oxo-anions such as PO_3^-. Synthesis and structural characterisation of imino counterparts of triiminophosphonates **III** and tetraiminophosphates **IV** have been reported very recently. Considering the vast variety of materials containing oxo-anions, there might be a great potential for imino analogues as building blocks in new materials.

Aza-P(V) derivatives such as phosphazenes **V** feature a chemically and thermally inert P–N- backbone. The high stability of these compounds has led to many specialised applications, particularly for poly(phosphazenes). Integration of both linking aza and terminal imino functions in P(V) ligands give linear monoanionic diiminophosphazenates **VI** and multianionic poly(imino)phosphazenates such as **VII** and **VIII**. The high negative charge and the extensive donor surface in multianionic systems facilitate extremely high metal loading per ligand entity. **VIII** is isoelectronic with the cyclotrisilicate ion $[Si_3O_9]^{6-}$, but features an organic periphery, which allows applications of highly charged ligands in solution.

P–N units in **I** and **V** act as electron withdrawing groups and enable α-deprotonation of P-alkyl and *ortho*-deprotonation of P-aryl groups. This has led to many interesting carbanionic ligand species, including the first structurally characterised methanediide derivatives. Carbanionic ligands stemming from α-deprotonation of iminophosphoranes are isoelectronic to corresponding imino–aza P(V) ligands.

Bonding distances within P–N frameworks of imino-, aza and imino–aza ligands are within a narrow range. This indicates similar bond order and equal distribution of charge throughout the P–N ligand structure. The P–N bond order decreases with increasing ratio of negative N-centres per phosphorus atom and increasing ligand charge Z. This is nicely illustrated in lithium complexes of the imino-series: **I** (N/P = 1:1, P–N = 154 pm (in **31**), $Z = 0$)), **II** (N/P = 2:1, P–N = 158 pm (in **43**), $Z = -1$)), **III** (N/P = 3:1, P–N = 162 pm (in **67**), $Z = -2$)) and **IV** (N/P = 4:1, P–N = 165 pm (in **70**), $Z = -3$)). Similar trends are observed in P–O bonds of corresponding oxo-anions of phosphorus. In imino–aza ligands the charge is distributed over N(imino) and N(aza) centres. Again P/N ratio and charge Z determine the average P–N bond distances, which are in the order **VI** (N/P = 1.5:1, P–N = 159 pm (in **88**), $Z = -1$), **VII** (N/P = 2:1, P–N = 162 pm (in **96a**), $Z = -4$) and **VIII** (N/P = 3:1, P–N = 165 pm (in **98a**), $Z = -6$).

Imino–aza-P(V) ligand systems **I**–**VIII** are assembled of only a few basic building blocks, which are the tetravalent phosphonium centre *P*, the divalent amido bridge *N* and the terminal R-group *R*. The ligand synthesis is straightforward and involves mainly two key methods: (i) Staudinger reaction and (ii) aminolysis of halo phosphoranes. Cage type ligands and extended 3-D frameworks, assembled from the same construction kit as **I**–**VIII**, were generated in high temperature reactions as solid-state materials. Low temperature routes to highly aggregated anions seem feasible taking into account the ease of preparation of molecular ligands **I**–**VIII**. In addition, R-groups on P- and N-atoms can be widely varied which allows the introduction of steric demand and additional donor sites. The combination of a kinetically very stable P–N-framework, a high metal loading capacity and a lipophilic ligand periphery promises many more interesting imino–aza-phosphorus(V) anions to come, both at the molecular level as well as in extended structures of inorganic/organic hybrid materials.

Acknowledgements

We thank EPSRC and The Royal Society for financial support.

References

[1] (a) F.T. Edelmann, Coord. Chem. Rev. 137 (1994) 403;
(b) P.J. Bailey, S. Pace, Coord. Chem. Rev. 214 (2001) 91;
(c) F. Rivals, A. Steiner, J. Chem. Soc. Chem. Commun. (2001) 2104;
(d) D.J. Brauer, H. Bürger, G.R. Liewald, J. Organomet. Chem. 308 (1986) 119.
[2] (a) M. Witt, H.W. Roesky, Chem. Rev. 94 (1994) 1163;
(b) M.A. Beswick, S.J. Kidd, M.A. Paver, P.R. Raithby, A. Steiner, D.S. Wright, Inorg. Chem. Commun. 2 (1999) 612;
(c) M.A. Beswick, N.L. Cromhout, C.N. Harmer, M.A. Paver, P.R. Raithby, M.-A. Rennie, A. Steiner, D.S. Wright, Inorg. Chem. 36 (1997) 1740;
(d) M.A. Beswick, M.E.G. Mosquera, D.S. Wright, J. Chem. Soc. Dalton Trans. (1998) 2437.
[3] R. Fleischer, D. Stalke, Coord. Chem. Rev. 176 (1998) 431.
[4] A.W. Johnson, Ylides and Imines of Phosphorus, Wiley, New York, 1993.
[5] J.K. Brask, T. Chivers, Angew. Chem. Int. Ed. Engl. 40 (2001) 3960.
[6] H. Staudinger, J. Meyer, Helv. Chim. Acta 2 (1919) 635.
[7] P. Imhoff, C.J. Elsevier, C.H. Stam, Inorg. Chim. Acta 175 (1990) 209.
[8] A. Müller, M. Krieger, B. Neumüller, K. Dehnicke, J. Magull, Z. Anorg. Allg. Chem. 623 (1997) 1081.
[9] A. Maurer, D. Fenske, J. Beck, W. Hiller, J. Strähle, E. Böhm, K. Dehnicke, Z. Naturforsch. B 43 (1988) 5.
[10] T. Miekisch, H.-J. Mai, R. Meyer zu Kocker, K. Dehnicke, J. Magull, H. Goesmann, Z. Anorg. Allg. Chem. 622 (1996) 583.
[11] D. Fenske, E. Böhm, K. Dehnicke, J. Strähle, Z. Naturforsch. B 43 (1988) 1.
[12] R. Meyer zu Kocker, G. Frenzen, B. Neumüller, K. Dehnicke, J. Magull, Z. Anorg. Allg. Chem. 620 (1994) 431.
[13] M. Krieger, K. Harms, J. Magull, K. Dehnicke, Z. Naturforsch. B50 (1995) 1215.
[14] T.P. Braun, P.A. Gutsch, H. Zimmer, Z. Naturforsch. B54 (1999) 858.
[15] H.R. Allcock, Phosphorus Nitrogen Compounds, Academic Press, New York, 1972.
[16] H. Schmidbaur, W. Wolfsberger, Chem. Ber. 100 (1967) 1000.
[17] K.V. Katti, R.G. Cavell, Inorg. Chem. 28 (1989) 413.
[18] R.G. Cavell, Curr. Sci. 78 (2000) 440.
[19] R.W. Reed, B. Santarsiero, R.G. Cavell, Inorg. Chem. 35 (1996) 4292.
[20] R. Appel, I. Ruppert, Z. Anorg. Allg. Chem. 406 (1974) 131.
[21] P. Imhoff, R. van Asselt, C.J. Elsevier, M.C. Zoutberg, C.H. Stam, Inorg. Chim. Acta 184 (1991) 73.
[22] M.W. Avis, K. Vrieze, H. Kooijman, N. Veldman, A.L. Spek, C.J. Elsevier, Inorg. Chem. 34 (1995) 4092.
[23] M.T. Reetz, E. Bohres, R. Goddard, J. Chem. Soc., Chem. Commun. (1998) 935.
[24] G. Boche, Angew. Chem. Int. Ed. Engl. 28 (1989) 277.
[25] F. López-Ortiz, E. Peláez-Arango, B. Tejerina, E. Pérez-Carreño, S. García-Granda, J. Am. Chem. Soc. 117 (1995) 9972.
[26] P.B. Hitchcock, M.F. Lappert, P.G.H. Uiterweerd, Z.-X. Wang, J. Chem. Soc., Dalton Trans. (1999) 3413.
[27] A. Müller, B. Neumüller, K. Dehnicke, Chem. Ber. 129 (1996) 253.
[28] A. Müller, B. Neumüller, K. Dehnicke, Angew. Chem. Int. Ed. Engl. 36 (1997) 2350.
[29] H.-J. Cristau, Chem. Rev. 94 (1994) 1299.
[30] P.B. Hitchcock, M.F. Lappert, Z.-X. Wang, J. Chem. Soc., Chem. Commun. (1997) 1113.
[31] A. Müller, B. Neumüller, K. Dehnicke, J. Magull, D. Fenske, Z. Anorg. Allg. Chem. 623 (1997) 1306.
[32] P. Imhoff, R. van Asselt, J.M. Ernsting, K. Vrieze, C.J. Elsevier, W.J.J. Smeets, A. Spek, A.P.M. Kentgens, Organometallics 12 (1993) 1523.
[33] R.P. Kamalesh Babu, K. Aparna, R. McDonald, R.G. Cavell, Organometallics 20 (2001) 1451.
[34] R.P. Kamalesh Babu, K. Aparna, R. McDonald, R.G. Cavell, Inorg. Chem. 39 (2000) 4981.
[35] K. Aparna, R. McDonald, M. Ferguson, R.G. Cavell, Organometallics 18 (1999) 4241.
[36] K. Aparna, R. McDonald, R.G. Cavell, Organometallics 18 (1999) 3775.
[37] C.M. Ong, D.W. Stephan, J. Am. Chem. Soc. 121 (1999) 2939.
[38] A. Kasani, R.P. Kamalesh Babu, R. McDonald, R.G. Cavell, Angew. Chem. Int. Ed. Engl. 38 (1999) 1483.
[39] K. Aparna, R. McDonald, R.G. Cavell, J. Am. Chem. Soc. 122 (2000) 9314.
[40] W.-P. Leung, Z.-X. Wang, H.-W. Li, T.C.W. Mak, Angew. Chem. Int. Ed. Engl. 40 (2001) 2501.
[41] R.G. Cavell, R.P. Kamalesh Babu, K. Aparna, J. Organomet. Chem. 617 (2001) 158.
[42] R.G. Cavell, R.P. Kamalesh Babu, A. Kasani, R. McDonald, J. Am. Chem. Soc. 121 (1999) 5805.
[43] R.P. Kamalesh Babu, R. McDonald, R.G. Cavell, Chem. Commun. (2000) 481.
[44] R.P. Kamalesh Babu, R. McDonald, R.G. Cavell, Organometallics 19 (2000) 3462.
[45] K. Aparna, M. Ferguson, R.G. Cavell, J. Am. Chem. Soc. 122 (2000) 727.
[46] A. Kasani, R. McDonald, R.G. Cavell, J. Chem. Soc., Chem. Commun. (1999) 1993.
[47] A. Steiner, D. Stalke, Angew. Chem. Int. Ed. Engl. 34 (1995) 1752.

[48] F. Weller, H. -C. Kang, W. Massa, T. Rubensthal, F. Kunkel, K. Dehnicke, Z. Naturforsch. B 50 (1995) 1050.
[49] H. Schmidbaur, W. Wolfsberger, Chem. Ber. 100 (1967) 1016.
[50] M.A. Leeson, B.K. Nicholson, M.R. Olson, J. Organomet. Chem. 579 (1999) 243.
[51] S. Wingerter, H. Gornitzka, G. Bertrand, D. Stalke, Eur. J. Inorg. Chem. (1999) 173.
[52] S. Wingerter, H. Gornitzka, R. Bertermann, S.K. Pandey, J. Rocha, D. Stalke, Organometallics 19 (2000) 3890.
[53] K.L. Paciorek, R.H. Kratzer, J. Org. Chem. 31 (1966) 2426.
[54] O.J. Scherer, G.J. Schieder, J. Organomet. Chem. 19 (1969) 315.
[55] H.-J. Cristau, C. Garcia, J. Kadoura, E. Torreilles, Phosphorus, Sulfur Silicon 49–50 (1990) 151.
[56] O.J. Scherer, G. Schnabl, T. Lenhard, Z. Anorg. Allg. Chem. 449 (1979) 167.
[57] A. Steiner, D. Stalke, Inorg. Chem. 32 (1993) 1977.
[58] R. Fleischer, D. Stalke, Inorg. Chem. 36 (1997) 2413.
[59] H. Schmidbaur, K. Schwirten, H.-H. Pickel, Chem. Ber. 102 (1969) 564.
[60] U. Kilimann, M. Noltemeyer, F.T. Edelmann, J. Organomet. Chem. 443 (1993) 35.
[61] A. Recknagel, A. Steiner, M. Noltemeyer, S. Brooker, D. Stalke, F.T. Edelmann, J. Organomet. Chem. 414 (1991) 327.
[62] A. Recknagel, M. Witt, F.T. Edelmann, J. Organomet. Chem. 371 (1989) C40.
[63] M. Witt, H.W. Roesky, D. Stalke, F. Pauer, T. Henkel, G.M. Sheldrick, J. Chem. Soc. Dalton Trans. (1989) 2173.
[64] M. Witt, D. Stalke, T. Henkel, H.W. Roesky, G.M. Sheldrick, J. Chem. Soc. Dalton Trans. (1991) 663.
[65] E. Müller, J. Müller, F. Olbrich, W. Brüser, W. Knapp, D. Abeln, F.T. Edelmann, Eur. J. Inorg. Chem. (1998) 87.
[66] R. Vollmerhaus, P. Shao, N.J. Taylor, S. Collins, Organometallics 18 (1999) 2731.
[67] H. Ackermann, O. Bock, U. Müller, K. Dehnicke, Z. Anorg. Allg. Chem. 626 (2000) 1854.
[68] B.F. Straub, F. Eisenträger, P. Hofmann, J. Chem. Soc., Chem. Commun. (1999) 2507.
[69] B.F. Straub, F. Rominger, P. Hofmann, J. Chem. Soc., Chem. Commun. (2000) 1611.
[70] S. Wingerter, M. Pfeiffer, A. Murso, C. Lustig, T. Stey, V. Chandrasekhar, D. Stalke, J. Am. Chem. Soc. 123 (2001) 1381.
[71] (a) A. Steiner, D. Stalke, J. Chem. Soc. Chem. Commun. (1993) 444;;
(b) A. Steiner, D. Stalke, Organometallics 14 (1995) 2422.
[72] P. Braunstein, R. Hasselbring, D. Stalke, New J. Chem. 20 (1996) 337.
[73] L.T. Burke, E. Hevia-Freire, R. Holland, J.C. Jeffrey, A.P. Leedham, C.A. Russell, A. Steiner, A. Zagorski, J. Chem. Soc., Chem. Commun. (2000) 1769.
[74] L.T. Burke, J.C. Jeffrey, A.P. Leedham, C.A. Russell, J. Chem., Soc. Dalton Trans. (2001) 423.
[75] P.J. Bailey, K.J. Grant, S. Parsons, Organometallics 17 (1998) 551.
[76] G.F. de la Fuente, J.E. Huheey, Phosphorus Sulfur Silicon 78 (1993) 23.
[77] O.J. Scherer, J. Kerth, Angew. Chem. Int. Ed. Engl. 23 (1984) 156.
[78] V.D. Romanenko, V.F. Shul'kin, V.V. Skopenko, A.N. Chernega, M.Y. Antipin, Y.T. Struchkov, I.E. Boldeskul, L.N. Markovskii, Z. Obshch. Khim. 55 (1985) 282.
[79] A.N. Chernega, M.Y. Antipin, Y.T. Struchkov, V.D. Romanenko, Koord. Khim. 15 (1989) 849.
[80] P.R. Raithby, C.A. Russell, A. Steiner, D.S. Wright, Angew. Chem. Int. Ed. Engl. 36 (1997) 649.
[81] J. Novosad, in: R.B. King (Ed.), Encyclopaedia of Inorganic Chemistry, vol. 6, Wiley, Chichester, 1994, p. 3144.
[82] A.P. Leedham, C.A. Russell, A. Steiner, S. Zacchini, unpublished results.
[83] E. Niecke, M. Frost, M. Nieger, V. von der Gönna, A. Ruban, W.W. Schoeller, Angew. Chem. Int. Ed. Engl. 33 (1994) 2111.
[84] (a) O.J. Scherer, J. Kerth, M.L. Ziegler, Angew. Chem. Int. Ed. Engl. 22 (1983) 503;
(b) O.J. Scherer, P. Quintus, W.S. Sheldrick, Chem. Ber. 120 (1987) 1183.
[85] D.F. Moser, C.J. Carrow, L. Stahl, R. Staples, J. Chem. Soc. Dalton Trans. (2001) 1246.
[86] G.R. Lief, C.J. Carrow, L. Stahl, R.J. Staples, Organometallics 20 (2001) 1629.
[87] R. Detsch, E. Niecke, M. Nieger, W.W. Schoeller, Chem. Ber. 125 (1992) 1119.
[88] E. Niecke, D. Gudat, Angew. Chem. Int. Ed. Engl. 30 (1991) 217.
[89] L. Stahl, Coord. Chem. Rev. 210 (2000) 203.
[90] H.R. Allcock, Chem. Rev. 72 (1972) 315.
[91] J.E. Mark, H.R. Allcock, R. West, Inorganic Polymers, Prentice-Hall, New Jersey, 1992.
[92] S.S. Krishnamurthy, A.C. Sau, Adv. Inorg. Chem. Radiochem. 21 (1978) 41.
[93] (a) C.W. Allen, Chem. Rev. 91 (1991) 119;
(b) C.W. Allen, in: I. Haiduc, D.B. Sowerby (Eds.), The Chemistry of Inorganic Homo and Heterocycles, Academic Press, London, 1989, p. 133.
[94] H.P. Calhoun, N.L. Paddock, J.N. Wingfield, Can. J. Chem. 53 (1975) 1765.
[95] (a) H.R. Allcock, J.L. Desorcie, G.H. Riding, Polyhedron 6 (1987) 119;
(b) V. Chandrasekhar, K.R. Justin Thomas, J. Appl. Organomet. Chem. 7 (1993) 1;
(c) V. Chandrasekhar, S. Nagendran, Chem. Soc. Rev. 30 (2001) 193.
[96] (a) R.W. Allen, J.P. O'Brien, H.R. Allcock, J. Am. Chem. Soc. 99 (1977) 3987;
(b) J.P. O'Brien, R.W. Allen, H.R. Allcock, Inorg. Chem. 18 (1979) 2230.
[97] J. Trotter, S.H. Whitlow, J. Chem. Soc. A (1970) 455.
[98] (a) W.C. Marsh, J. Trotter, J. Chem. Soc. A (1971) 1482;;
(b) W. Harrison, J. Trotter, J. Chem. Soc., Dalton Trans. (1973) 61;;
(c) N.L. Paddock, T.N. Ranganathan, S.J. Rettig, R.D. Sharma, J. Trotter, Can. J. Chem. 59 (1981) 2429.
[99] H.P. Calhoun, N.L. Paddock, J. Trotter, J. Chem. Soc., Dalton Trans. (1973) 2708.
[100] A. Chandrasekaran, S.S. Krishnamurthy, M. Nethaji, Inorg. Chem. 33 (1994) 3085.
[101] K.R. Justin Thomas, V. Chandrasekhar, P.S. Pal, S.R. Scott, R. Hallford, A.W. Cordes, Inorg. Chem. 32 (1993) 606.
[102] E.W. Ainscough, A.M. Brodie, C.V. Depree, J. Chem. Soc., Dalton Trans. (1999) 4123.
[103] U. Diefenbach, M. Kretschmann, B. Stromburg, Chem. Ber. 129 (1996) 1573.
[104] H.R. Allcock, R.W. Allen, J.P. O'Brien, J. Am. Chem. Soc. 99 (1977) 3984.
[105] H.R. Allcock, Acc. Chem. Res. 12 (1979) 352.
[106] H.R. Allcock, S.J.M. O'Conner, D.L. Olmeijer, M.E. Napierala, C.G. Cameron, Macromolecules 29 (1996) 7544.
[107] C.H. Walker, J.V. St. John, P. Wisian-Neilson, J. Am. Chem. Soc. 123 (2001) 3846.
[108] K.D. Gallicano, R.T. Oakley, N.L. Paddock, R.D. Sharma, Can. J. Chem. 59 (1981) 2654.
[109] (a) P. Wisian-Neilson, R.R. Ford, R.H. Neilson, A.K. Roy, Macromolecules 19 (1986) 2091;
(b) R.H. Neilson, P. Wisian-Neilson, Chem. Rev. 88 (1988) 541.

[110] A. Steiner, G.T. Lawson, B. Walfort, D. Leusser, D. Stalke, J. Chem. Soc., Dalton Trans. (2001) 219.
[111] (a) I.I. Bezman, J.H. Smalley, Chem. Ind. (1960) 839;;
(b) A. Schmidpeter, C. Weingand, E. Hafner-Roll, Z. Naturforsch. B 24 (1969) 799;
(c) S.K. Pandey, H.W. Roesky, D. Stalke, A. Steiner, H.-G. Schmidt, M. Noltemeyer, Phosphorus Sulfur Silicon 84 (1993) 231.
[112] S.K. Pandey, R. Hasselbring, A. Steiner, D. Stalke, H.W. Roesky, Polyhedron 12 (1993) 2941.
[113] R. Hasselbring, H.W. Roesky, A. Heine, D. Stalke, G.M. Sheldrick, Z. Naturforsch. B 49 (1994) 43.
[114] J.F. van der Maelen Uria, S.K. Pandey, H.W. Roesky, G.M. Sheldrick, Acta Crystallogr. C 50 (1994) 671.
[115] R. Hasselbring, S.K. Pandey, H.W. Roesky, D. Stalke, A. Steiner, J. Chem. Soc., Dalton Trans. (1993) 3447.
[116] S.K. Pandey, A. Steiner, H.W. Roesky, D. Stalke, Angew. Chem. Int. Ed. Engl. 32 (1993) 596.
[117] S.K. Pandey, A. Steiner, H.W. Roesky, D. Stalke, Inorg. Chem. 32 (1993) 5444.
[118] (a) S.K. Ray, R.A. Shaw, J. Chem. Soc. (1961) 872.;
(b) B. Grushkin, A.J. Berlin, J.L. McClanahan, R.G. Rice, Inorg. Chem. 5 (1966) 172.
[119] A. Steiner, D.S. Wright, J. Chem. Soc., Chem. Commun. (1997) 283.
[120] G.J. Bullen, P.R. Mallison, J. Chem. Soc., Chem. Commun. (1969) 691.
[121] A. Steiner, D.S. Wright, Angew. Chem. Int. Ed. Engl. 35 (1996) 636.
[122] G.T. Lawson, F. Rivals, M. Tascher, C. Jacob, J.F. Bickley, A. Steiner, Chem. Commun. (2000) 341.
[123] G.T. Lawson, A. Steiner, Organometallics, in preparation.
[124] G.T. Lawson, C. Jacob, A. Steiner, Eur. J. Inorg. Chem. (1999) 1881.
[125] F. Rivals, A. Steiner, J. Chem. Soc., Chem. Commun. (2001) 1426.
[126] F. Rivals, A. Steiner, unpublished results.
[127] F. Golinski, H. Jacobs, Z. Anorg. Allg. Chem. 621 (1995) 29.
[128] W. Schnick, Angew. Chem. Int. Ed. Engl. 32 (1993) 806.
[129] W. Schnick, J. Lücke, Z. Anorg. Allg. Chem. 588 (1990) 19.
[130] W. Schnick, J. Lücke, Angew. Chem. Int. Ed. Engl. 31 (1992) 213.
[131] (a) K. Dehnicke, F. Weller, Coord. Chem. Rev. 158 (1997) 103;
(b) K. Dehnicke, J. Strähle, Polyhedron 8 (1989) 707;
(c) K. Dehnicke, M. Krieger, W. Massa, Coord. Chem. Rev. 182 (1999) 19.
[132] H.W. Roesky, Synlett 1990, 651.